

## January 2024 ERRATA for *Mechanistic–Empirical Pavement Design Guide*, 3rd Edition, PE Exam Edition (MEPDG-3-PE)

January 2024

Dear Customer:

AASHTO has issued a third erratum, which includes technical revisions, for the *Mechanistic–Empirical Pavement Design Guide*, 3rd Edition, PE Exam Edition (MEPDG-3-PE).

In the event that you need to download this file again, it can be found on AASHTO’s website at:

<https://downloads.transportation.org/MEPDG-3PE-Errata.pdf>

The new changes in this erratum are detailed in the table under the “January 2024” heading. No special type style has been used in the text so that the content is easier to read; the “October 2023” changes were extensive. Pages with the new changes have a gray box in the page header reading as follows:

January 2024 Errata

The previous changes are detailed in the table under the “October 2023” and “August 2022” headings. These pages have a gray box in the page header reading that may read one of three ways:

October 2023 Errata

October 2023 Errata  
August 2022 Errata

August 2022 Errata

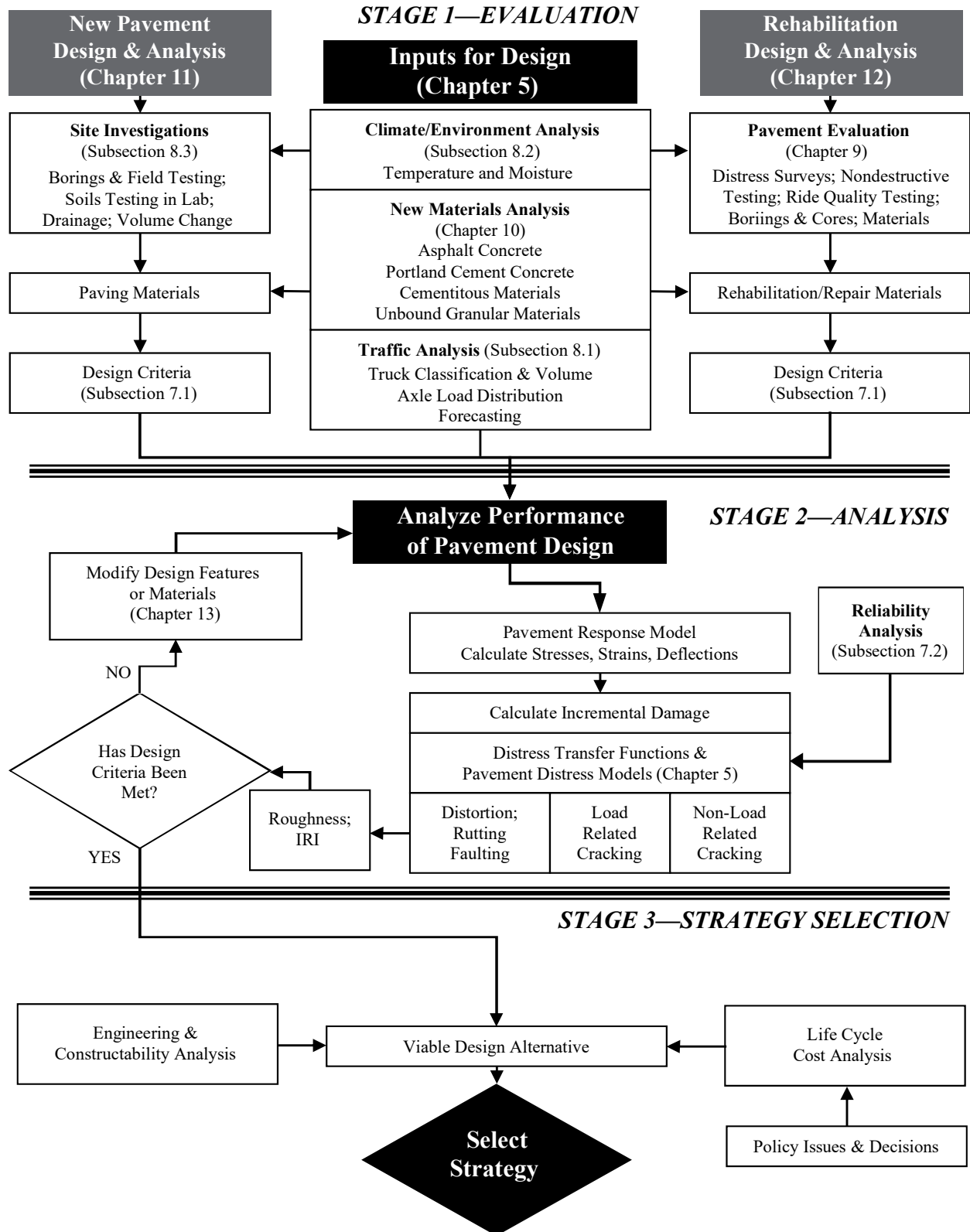
AASHTO staff sincerely apologizes for any inconvenience.

This page intentionally left blank.

**List of Errata for AASHTO Mechanistic–Empirical Pavement Design Guide, 3rd Edition,  
PE Exam Edition (MEPDG-3-PE)**

Original Page	Section	Existing Text	Corrected Text
<b>January 2024</b>			
224	Table 13-3	In row 1, column 2 on this page, the first bullet should be part of the note.	<p>Table reads as follows:</p> <p><i>Note:</i> It is recommended to not use the surface-initiated crack prediction equation as a design criterion until the critical pavement response parameter and prediction methodology has been verified. Refer to Chapter 3.</p> <p>The cumulative damage and longitudinal cracking transfer function (Equations 5-5 and 5-8) should be used with caution when making design decisions (in terms of longitudinal cracking, or top-down cracking) regarding the adequacy of a trial design.</p>
<b>October 2023</b>			
vi	Table P-1	In the Coefficient of Thermal Expansion (CTE) row, AASHTOWare columns, the coefficients both are shown as 5.2.	The coefficients both should be shown as 4.3.
viii		In the Calibration Coefficient in the Rigid Pavement Punchout Prediction Model rows, MEPDG version 1.1 column, the coefficients are shown as $A_{PO}$ , $\alpha_{PO}$ , and $\beta_{PO}$ .	The coefficients should be shown as $A_{PO}$ , $\alpha_{PO}$ , and $\beta_{PO}$ .
xiv	List of Figures	Some Chapter 5 page numbers were incorrect.	Corrected page numbers for Figures 5-15, 5-17, 5-18, and 5-20.
3	Figure 1-1	Under Inputs for Design, the Traffic Analysis box is missing a vertical connector line.	Figure 1-1 is corrected as shown on the next page.

List of Errata for *AASHTO Mechanistic–Empirical Pavement Design Guide, 3rd Edition, PE Exam Edition (MEPDG-3-PE)*



List of Errata for *AASHTO Mechanistic–Empirical Pavement Design Guide*, 3rd Edition,  
PE Exam Edition (MEPDG-3-PE)

Original Page	Section	Existing Text	Corrected Text
<b>October 2023</b>			
6	1.2	Step 3 following Figure 1-1 is missing a cautionary statement.	Step 3 has been revised to end with the following:  <i>A caution to the designer</i> —Some of the input parameters are interrelated; changing one parameter may affect the value of another input parameter. The designer should use caution in making changes in individual parameters.
41	Table 5-1	In the Truck Traffic row, most column 1 content should be in column 2 and most column 2 content should be in column 3.	Table 5-1 has been revised as shown on the next page.
		In the All Materials row, most column 1 content should be in column 2 and most column 2 content should be in column 3.	
		In the All Materials row, “capacitydentifce” should be “capacity, surface”.	

List of Errata for *AASHTO Mechanistic–Empirical Pavement Design Guide*, 3rd Edition, PE Exam Edition (MEPDG-3-PE)

Input Group		Input Parameter	Recalibration Input Level Used
Truck Traffic		Axle load distributions (single, tandem, tridem)	Level 1
		Truck volume distribution	Level 1
		Lane and directional truck distributions	Level 1
		Tire pressure	Level 3, default
		Axle configuration, tire spacing	Level 3, default
		Truck wander	Level 3, default
Climate		Temperature, wind speed, cloud cover, precipitation, relative humidity	Level 1 weather stations
Material Properties	Unbound Layers and Subgrade	Resilient modulus—all unbound layers	Level 1; backcalculation
		Classification and volumetric properties	Level 1
		Moisture-density relationships	Level 1
		Soil-water characteristic relationships	Level 3, defaults
		Saturated hydraulic conductivity	Level 3, defaults
	AC	AC dynamic modulus	Level 3, defaults
		AC creep compliance and indirect tensile strength	Levels 1, 2, and 3
		Volumetric properties	Level 1
		AC coefficient of thermal expansion	Level 3, default
	PCC	PCC elastic modulus	Level 1
		PCC flexural strength	Level 1
		PCC indirect tensile strength (CRCP only)	Level 2
		PCC coefficient of thermal expansion	Level 1
All Materials		Unit weight	Level 1
		Poisson’s ratio	Level 3, default
		Other thermal properties—conductivity, heat capacity, surface absorptivity	Level 3, defaults
Existing Pavement		Condition of existing layers	Levels 1 and 2

List of Errata for *AASHTO Mechanistic–Empirical Pavement Design Guide*, 3rd Edition,  
PE Exam Edition (MEPDG-3-PE)

Original Page	Section	Existing Text	Corrected Text
<b>October 2023</b>			
45	Eq. 5-2d	Equation 5-2d wrongly includes “= 0.0075”.	The correct equation is as follows: $C_o = Ln \left( \frac{a_1 M_r^{b_1}}{a_0 M_r^{b_0}} \right)$
46	5.3.3	<ul style="list-style-type: none"> <li>The first paragraph under “Asphalt Concrete Layers” is incorrect.</li> </ul>	<p>The first paragraph has been revised as follows:</p> <p>Two types of load-related cracks are predicted by the MEPDG: alligator cracking and longitudinal cracking. The MEPDG assumes that alligator, or area cracks, initiate at the bottom of the AC layers and propagate to the surface with continued truck traffic, while longitudinal cracks are assumed to initiate at the surface.</p> <p><i>For bottom-up or alligator cracking:</i> The allowable number of axle load applications needed for the incremental damage index approach to predict bottom-up cracks is shown in Equation 5-4a.</p>
		<ul style="list-style-type: none"> <li>Equation 5-4a is incorrect.</li> </ul>	<p>The equation reads as follows:</p> $N_{f-AC} = k_{f1}(C)(C_H)\beta_{f1}(\epsilon_t)^{-k_{f2}\beta_{f2}}(E_{AC})^{-k_{f3}\beta_{f3}}$
47		<ul style="list-style-type: none"> <li>Following Equation 5-4d, the notation for <math>C_H</math> is incorrect, including row 2 column 2 of the table.</li> </ul>	<p>The notation reads as follows: <math>C_H</math> = Thickness correction term ... <math display="block">1/(-0.046908H_{AC}^3 + 0.729644H_{AC}^2 - 0.635578H_{AC} - 1.555892)</math></p>
		<ul style="list-style-type: none"> <li>Equations 5-4e and 5-4f should not be included.</li> </ul>	<p>Equations 5-4e and Equation 5-4f have been deleted. The subheader between them has been moved.</p>
48		<ul style="list-style-type: none"> <li>In the paragraph before Equation 5-6a, “and length of longitudinal cracking” should not be included.</li> </ul>	<p>The first sentence of the paragraph reads as follows:</p> <p>The area of alligator cracking is calculated from the total damage over time (Equation 5-5) using different transfer functions.</p>
53	5.3.4	Equations 5-12b, 5-12d, and 5-12f are incorrect.	<p>The equations read as follows:</p> $S_e \text{ (Level 1; MAAT > 57°F)} = 0.14(TC) + 343$ $S_e \text{ (Level 2; MAAT > 57°F)} = 0.20(TC) + 343$

List of Errata for *AASHTO Mechanistic–Empirical Pavement Design Guide*, 3rd Edition, PE Exam Edition (MEPDG-3-PE)

Original Page	Section	Existing Text	Corrected Text
<b>October 2023</b>			
			$S_e$ (Level 3; $MAAT > 57^\circ\text{F}$ ) = 0.2386( $TC$ ) + 343
59	Table 5-2	Table 5-2 coefficients are incorrect.	Table 5-2 coefficients have been corrected as shown below in red.

Calibration Coefficients	Pavement Type				
	AC over AC	AC over Intact JPCP	AC over Intact CRCP or Fractured JPCP	Semi-Rigid	AC over Semi-Rigid
$k_1$	0.012	0.012	0.012	0.45	0.012
$k_2$	0.005	0.005	0.0002	0.05	0.005
$k_3$	1.00	1.00	0.1	1.0	1.0
$C_1$	3.22	3.22	3.22	0.1	3.22
$C_2$	25.7	25.7	25.7	0.9809	25.7
$C_3$	0.1	0.1	0.1	0.19	0.1
$C_4$	133.4	133.4	133.4	165.3	133.4
$C_5$	-72.4	-72.4	-72.4	-5.1048	-72.4

Original Page	Section	Existing Text	Corrected Text
<b>October 2023</b>			
63	5.4.1	The second variable in the where list for Equation 5-20a is incorrect.	The variable reads as follows: $n_{i,j,k,\dots}$
70	5.4.2	In the paragraph before Equations 5-28a and 5-28b, the variable is incorrect.	The correct variable is $\Delta s$ .
75	5.4.3	Equation 5-33 is incorrect.	The equation reads as follows: $CW = \text{Max} \left[ L \left( \epsilon_{shr} + \alpha_{PCC} \Delta T_s - \frac{c_2 f_{\sigma long}}{E_{PCC}} \right) (C_c) 1000 \right]$
78	5.4.4	Equation 5-37 is incorrect.	The equation reads as follows: $LCRK = \frac{1}{1 + C_4 (DI_F)^{C_5}}$

List of Errata for *AASHTO Mechanistic–Empirical Pavement Design Guide*, 3rd Edition,  
PE Exam Edition (MEPDG-3-PE)

Original Page	Section	Existing Text	Corrected Text
<b>October 2023</b>			
81	5.4.5	Equation 5-41a is incorrect.	The equation reads as follows: $IRI = IRI_i + J1 * CRK + J2 * SPALL + J3 * TFAULT + J4 * SF$
146	Table 10-3	In rows 1 and 2, columns 1 and 2 of Table 10-3, “EHMA” and “EAC” are incorrect.	The table shows “ $E_{HMA}$ ” and “ $E_{AC}$ ”.
148		In the embedded table in row 1 of Table 10-3, “ $\mu_{typical}$ ” is incorrect.	The table shows “ $\mu_{typical}$ ”
153	Table 10-5	In Row 1 column 2 of Table 10-5, “ $T_z$ ” is incorrect.	The table shows “ $T_z$ ”.
155	Table 10-7	In Table 10-7, “ $E = 57000(f'_c)0.5$ ” is incorrect.	The table shows the following: $E = 57000(f'_c)^{0.5}$
157	Table 10-9	In row 1, column 2 of Table 10-9, paragraph breaks are missing between the options.	Table reads as follows:  Two Options:  Regression coefficients $k_1, k_2, k_3$ for the generalized constitutive model that defines resilient modulus as a function of stress state and regressed from laboratory resilient modulus tests.  Determine the average design resilient modulus for the expected in-place stress state from laboratory resilient modulus tests.
211	Table 12-13	In row 1, Faulting, column 2, a bullet point is missing.	The following appears as the fourth of five bullets:  <ul style="list-style-type: none"> <li>• <b>Decrease joint spacing.</b> This is applicable to JPCP overlays over existing flexible pavements and unbonded JPCP overlays. Shorter joint spacing generally results in smaller joint openings, making aggregate interlock more effective and increasing joint LTE.</li> </ul>
235	Index	Page numbers; based on the original third edition.	Added the following at the top of the first index page:  <b>Note:</b> Index page numbers are based on the original third edition; they have not been updated to reflect any errata repagination.

List of Errata for *AASHTO Mechanistic–Empirical Pavement Design Guide*, 3rd Edition, PE Exam Edition (MEPDG-3-PE)

Original Page	Section	Existing Text	Corrected Text
<b>August 2022</b>			
67	5.4.2	Equation 5-23c is incorrect.	$FAULTMAX_i = FAULTMAX_{i-1} + C_7 \times \frac{\sum_{j=1}^m DE_j}{10^6} \times \text{Log}(1 + C_5 \times 5.0^{EROD})^{C_6}$
74	5.4.3	Equation 5-30 is incorrect.	$PO = \frac{C_3}{1 + C_4 (DI_{PO})^{C_5}}$
79	5.4.4	The equation and graph in Figure 5-19 are incorrect.	The equation and graph in Figure 5-19 have been revised to match Equation 5-37.
127	9.2.7	At the end of Table 9-8’s caption, add “(21)” (citing reference 21 in Chapter 2).	<b>Table 9-8.</b> Models Relating Material Index and Strength Properties to $M_r$ (21)
	Table 9-8	In the R-value row of Table 9-8, delete “(22)”.	$M_r = 1155 + 555R$ $M_r, \text{ psi}$
127	Table 9-8	In the AASHTO layer coefficient row of Table 9-8, change “3000” to “30,000” and delete “(22)”.	$M_r = 30,000 \left( \frac{a_i}{0.14} \right)$ $M_r, \text{ psi}$
		In the PI and gradation row of Table 9-8, delete “(See Appendix CC)”.	$CBR = \frac{75}{1 + 0.278(P_{200}PI)}$

List of Errata for *AASHTO Mechanistic–Empirical Pavement Design Guide*, 3rd Edition, PE Exam Edition (MEPDG-3-PE)

Original Page	Section	Existing Text	Corrected Text																								
<b>August 2022</b>																											
152	10.4	In Table 10-5, the coefficient of thermal expansion values and the default are incorrect.	<table border="1" data-bbox="824 426 1401 1041"> <thead> <tr> <th data-bbox="824 426 1162 569">Aggregates Type</th> <th data-bbox="1162 426 1401 569">Coefficient of Thermal Expansion (10<sup>-6</sup>/°F)</th> </tr> </thead> <tbody> <tr> <td data-bbox="824 569 1162 611">Andesite</td> <td data-bbox="1162 569 1401 611">4.3</td> </tr> <tr> <td data-bbox="824 611 1162 653">Basalt</td> <td data-bbox="1162 611 1401 653">4.3</td> </tr> <tr> <td data-bbox="824 653 1162 695">Diabase</td> <td data-bbox="1162 653 1401 695">4.6</td> </tr> <tr> <td data-bbox="824 695 1162 737">Gabbro</td> <td data-bbox="1162 695 1401 737">4.4</td> </tr> <tr> <td data-bbox="824 737 1162 779">Granite</td> <td data-bbox="1162 737 1401 779">4.7</td> </tr> <tr> <td data-bbox="824 779 1162 821">Schist</td> <td data-bbox="1162 779 1401 821">4.4</td> </tr> <tr> <td data-bbox="824 821 1162 863">Dolomite</td> <td data-bbox="1162 821 1401 863">5.0</td> </tr> <tr> <td data-bbox="824 863 1162 905">Limestone</td> <td data-bbox="1162 863 1401 905">4.3</td> </tr> <tr> <td data-bbox="824 905 1162 947">Quartzite</td> <td data-bbox="1162 905 1401 947">5.2</td> </tr> <tr> <td data-bbox="824 947 1162 989">Sandstone</td> <td data-bbox="1162 947 1401 989">5.3</td> </tr> <tr> <td data-bbox="824 989 1162 1031">Expanded shale</td> <td data-bbox="1162 989 1401 1031">4.5</td> </tr> </tbody> </table> <p data-bbox="824 1077 1471 1142">Where coarse aggregate type is unknown, use MEPDG default value of 4.4*10<sup>-6</sup>/°F.</p>	Aggregates Type	Coefficient of Thermal Expansion (10 <sup>-6</sup> /°F)	Andesite	4.3	Basalt	4.3	Diabase	4.6	Gabbro	4.4	Granite	4.7	Schist	4.4	Dolomite	5.0	Limestone	4.3	Quartzite	5.2	Sandstone	5.3	Expanded shale	4.5
Aggregates Type	Coefficient of Thermal Expansion (10 <sup>-6</sup> /°F)																										
Andesite	4.3																										
Basalt	4.3																										
Diabase	4.6																										
Gabbro	4.4																										
Granite	4.7																										
Schist	4.4																										
Dolomite	5.0																										
Limestone	4.3																										
Quartzite	5.2																										
Sandstone	5.3																										
Expanded shale	4.5																										
207	12.3.4	<p data-bbox="381 1150 760 1182"><i>Performance Prediction Models</i></p> <p data-bbox="381 1186 797 1478">The globally calibrated performance models for new pavements apply to rehabilitation design, but with one exception—the JPCP CPR faulting prediction model has slightly different coefficients than the corresponding one for new or reconstructed JPCP.</p>	<p data-bbox="824 1150 1203 1182"><i>Performance Prediction Models</i></p> <p data-bbox="824 1186 1438 1247">The globally calibrated performance models for new pavements apply to rehabilitation design.</p>																								

List of Errata for *AASHTO Mechanistic–Empirical Pavement Design Guide*, 3rd Edition, PE Exam Edition (MEPDG-3-PE)

Original Page	Section	Existing Text	Corrected Text
<b>August 2022</b>			
209	12.3.4	<p>In the JPCP overlay over existing flexible pavement row of Table 12-12, the recommendations read as follows:</p> <p>Selection of design features for the JPCP overlay (including shoulder type and slab width) is similar to that outlined for new or reconstructed design in Chapter 10. Condition of existing flexible pavement is rated as Excellent, Good, Fair, Poor, or Very Poor, as defined in Table 12-10. These ratings will result in adjustments to the dynamic modulus, <math>E_{HMA}</math>, of the existing AC layer that now becomes the base course. Full friction should be input over the full design life of the concrete overlay.</p>	<p>The corrected recommendations read as follows:</p> <p>Selection of design features for the JPCP overlay (including shoulder type and slab width) is similar to that outlined for new or reconstructed design in Chapter 10. Condition of existing flexible pavement is characterized using one of the three hierarchical input levels:</p> <ul style="list-style-type: none"> <li>• Level 1 rehabilitation calculates the existing damage based on the FWD back-calculated modulus.</li> <li>• Level 2 calculates the damage based on the existing fatigue cracking from a visual distress survey.</li> <li>• Level 3 calculates the damage based on a condition rating as Excellent, Good, Fair, Poor, or Very Poor, as defined in Table 12-10.</li> </ul> <p>For all rehabilitation levels, the dynamic modulus, <math>E_{HMS}</math>, is adjusted to reflect the magnitude of damage within the existing asphalt layers. The existing AC layer now becomes the base course in the analysis mod. Full friction should be input over the full design life of the concrete overlay.</p>

## Preface

This document or manual of practice describes a pavement design methodology that is based on engineering mechanics and has been validated with extensive road test performance data. This methodology is termed mechanistic-empirical (ME) pavement design, and it represents a major change from the pavement design methods in practice today.

Interested agencies have already begun implementation activities through staff training, collection of input data (materials library, traffic library, etc.), acquiring of test equipment, and preparation of field sections for local calibration. This manual, referred to as the Mechanistic-Empirical Pavement Design Guide (MEPDG), presents the information necessary for pavement design engineers to start using the ME-based design and analysis method. The software supporting this method is called Pavement ME Design<sup>®</sup> and is commercially available through AASHTOWare. The software is referred to in this document as PMED.

Multiple enhancements have been made to the AASHTOWare PMED based on completed research projects sponsored by the National Cooperative Highway Research Program (NCHRP) and the Federal Highway Administration (FHWA). In addition, revisions to the software were based on evaluations performed by State Highway Agencies and others in the Community of Practice. The third edition of the MEPDG Manual of Practice was prepared so the manual was consistent with the enhanced features and models included in the software through 2018.

The following table (Table P-1) summarizes the key differences noted between the format and calibration factors used in the MEPDG version 1.1 software, the AASHTOWare Pavement ME Design software version 2.3.1, and version 2.5.3 software.

**Table P-1.** Summary of Key Differences in Software Format and Calibration Factors

Format, Transfer Functions, and Calibration Coefficients		MEPDG version 1.1	AASHTOWare Pavement ME Design version 2.3.1	AASHTOWare Pavement ME Design version 2.5.3
Output Format		Excel-based	PDF- and Excel-based	PDF- and Excel-based
Climatic Input Data and if Included in Output Summary		Data from Ground-Based Weather Stations; output summary not included	Data from NARR database for rigid and flexible pavements; output summary included	Data from NARR database for rigid pavements and MERRA2 database for flexible and semi-rigid pavements; output summary included
Axle Configuration Data in Output Summary		Not included	Included	Included
Special Axle Load Configuration		Included	Not included	Not included
Reflection Cracking Transfer Function		Empirical regression equation included	ME-based fracture mechanics model included	ME-based fracture mechanics model included
Coefficient of Thermal Expansion (CTE)		CTE for Basalt of 4.6	CTE for Basalt of 4.3	CTE for Basalt of 4.3
PCC Zero Stress Temperature		PCC Zero Stress Temperature (60°–120°F)	PCC Set Temperature (70°–212°F)	PCC Set Temperature (70°–212°F)
Heat Capacity of Asphalt Pavement		Default value of 0.23 BTU/lb-°F	Default value of 0.28 BTU/lb-°F	Default value of 0.28 BTU/lb-°F
Thermal Conductivity of Asphalt Pavement		Default value of 0.67 BTU/(ft)(hr)(F)	Default value of 1.25 BTU/(ft)(hr)(F)	Default value of 1.25 BTU/(ft)(hr)(F)
Surface Shortwave Absorptivity		Default value of 0.95	Default value of 0.85	Default value of 0.85
Global Model Coefficient for Unbound Materials and Soils in Flexible Pavement Subgrade Rutting Model	Aggregate Base	$k_{s1}$ of 1.673	$k_{s1}$ of 2.03	$k_{s1}$ of 0.965
	Coarse-Grained Soil			$k_{s1}$ of 0.965
	Sand Soil			$k_{s1}$ of 0.635
	Fine-Grained Soil	$k_{s1}$ of 1.35	$k_{s1}$ of 1.35	$k_{s1}$ of 0.675

Continued on next page.

**Table P-1.** Summary of Key Differences in Software Format and Calibration Factors, *continued*

Format, Transfer Functions, and Calibration Coefficients		MEPDG version 1.1	AASHTOWare Pavement ME Design version 2.3.1	AASHTOWare Pavement ME Design version 2.5.3
Global Local Calibration or Field Adjustment Constant for Unbound Materials and Soils in Flexible Pavement Subgrade Rutting Model	Aggregate Base	1.0	1.0	1.0
	Coarse-Grained Soil			1.0
	Sand Soil			1.0
	Fine-Grained Soil			1.0
Global Laboratory-Derived Model Coefficients in the Fatigue Cracking Prediction Model in Flexible Pavement		$k_{s1}$ of 0.007566	$k_{s1}$ of 0.007566	$k_{s1}$ of 3.75
		$k_{s2}$ of -3.9492	$k_{s2}$ of 3.9492	$k_{s2}$ of 2.87
		$k_{s3}$ of -1.281	$k_{s3}$ of 1.281	$k_{s3}$ of 1.46
Global Local Calibration or Field-Adjustment Constants for Fatigue Cracking Prediction Model in Flexible Pavement		$\beta_1$ of 1.0	$\beta_1$ of 1.0	AC thickness dependent; see Chapter 5
		$\beta_2$ of 1.0	$\beta_2$ of 1.0	$\beta_2$ of 1.38
		$\beta_3$ of 1.0	$\beta_3$ of 1.0	$\beta_3$ of 0.88
Global Bottom-Up Alligator Cracking Transfer Function Coefficients		$C_1$ of 1.0	$C_1$ of 1.0	1.31
		$C_2$ of 1.0	$C_2$ of 1.0	AC thickness dependent; see Chapter 5
Global Calibration or Field-Adjustment Coefficient in the Transverse Cracking Model for AC		$k_t$ (Level 1) of 5.0	$k_t$ (Level 1) of 1.5	$k_s$ (Level 1) is Mean Annual Air Temperature (MAAT) dependent; see Chapter 5.
		$k_t$ (Level 2) of 1.5	$k_t$ (Level 2) of 0.5	$k_s$ (Level 2) is MAAT dependent; see Chapter 5.
		$k_t$ (Level 3) of 3.0	$k_t$ (Level 3) of 1.5	$k_s$ (Level 3) is MAAT dependent; see Chapter 5.
Global Laboratory Derived Model Coefficients in the Rut Depth Prediction Model		$k_1$ of -3.35412	$k_1$ of -3.35412	$k_1$ of -2.45
		$k_{2r}$ of 0.4791	$k_2$ of 1.5606	$k_2$ of 3.01
		$k_{3r}$ of 1.5606	$k_3$ of 0.4791	$k_3$ of 0.22

Continued on next page.

**Table P-1.** Summary of Key Differences in Software Format and Calibration Factors, *continued*

Format, Transfer Functions, and Calibration Coefficients	MEPDG version 1.1	AASHTOWare Pavement ME Design version 2.3.1	AASHTOWare Pavement ME Design version 2.5.3
Global Local Calibration or Field Adjustment Coefficients in the Rut Depth Prediction Model	$\beta_1$ of 1.0	$\beta_1$ of 1.0	$\beta_1$ of 0.40
	$\beta_2$ of 1.0	$\beta_2$ of 1.0	$\beta_2$ of 0.52
	$\beta_3$ of 1.0	$\beta_3$ of 1.0	$\beta_3$ of 1.36
Calibration Coefficients in the Rigid Pavement Cracking Prediction Model	$C_4$ of 1.0	$C_4$ of 0.52	$C_4$ of 0.52
	$C_5$ of -1.98	$C_5$ of -2.17	$C_5$ of -2.17
Calibration Coefficients in the Rigid Pavement Faulting Prediction Model	$C_1$ of 1.29	$C_1$ of 1.0184	$C_1$ of 0.595
	$C_2$ of 1.1	$C_2$ of 0.91656	$C_2$ of 1.636
	$C_3$ of 0.001725	$C_3$ of 0.0021848	$C_3$ of 0.00217
	$C_4$ of 0.0008	$C_4$ of 0.0008837	$C_4$ of 0.00444
	$C_6$ of 0.4	$C_6$ of 0.47	$C_6$ of 0.47
Calibration Coefficient in the Rigid Pavement Punchout Prediction Model	$C_7$ of 1.2	$C_7$ of 1.83312	$C_7$ of 7.3
	$A_{PO}$ of 195.789	$C_3$ of 107.73	$C_3$ of 107.73
	$\alpha_{PO}$ of 19.8947	$C_4$ of 2.476	$C_4$ of 2.475
Calibration Coefficients in the Short JPCP Overlay Longitudinal Cracking Prediction Model	$\beta_{PO}$ of -0.526316	$C_5$ of -0.785	$C_5$ of -0.785
	Excluded	$C_4$ of 0.4	$C_4$ of 0.4
		$C_5$ of -2.21	$C_5$ of -2.21

## List of Figures

Figure 1-1.	Conceptual Flow Chart of the Three-Stage Design/Analysis Process for AASHTOWare PMED . . . . .	3
Figure 1-2.	Typical Differences between Empirical Design Procedures and an Integrated ME Design System, in Terms of AC Mixture Characterization . . . . .	4
Figure 1-3.	Typical Differences between Empirical Design Procedures and an Integrated ME Design System, in Terms of PCC-Mixture Characterization. . . . .	5
Figure 1-4.	Flow Chart of the Steps That Are More Policy Decision Related and Needed to Complete an Analysis of a Trial Design Strategy . . . . .	7
Figure 1-5.	Flow Chart of the Steps Needed to Complete an Analysis of a Trial Design Strategy. . . . .	8
Figure 3-1.	New (Including Lane Reconstruction) Flexible Pavement Design Strategies That Can Be Simulated with the AASHTOWare PMED . . . . .	21
Figure 3-2.	AC Overlay Design Strategies of Flexible, Semi-Rigid, and Rigid Pavements That Can Be Simulated with the AASHTOWare PMED . . . . .	21
Figure 3-3.	New (Including Lane Reconstruction) Rigid Pavement Design Strategies That Can Be Simulated with the AASHTOWare PMED . . . . .	25
Figure 3-4.	PCC Overlay Design Strategies of Flexible, Semi-Rigid, and Rigid Pavements That Can Be Simulated with the AASHTOWare PMED . . . . .	26
Figure 5-1.	Graphical Illustration of the Five Temperature Quintiles Used in the MEPDG to Determine AC Mixture Properties for Load Related Distresses. . . . .	42
Figure 5-2.	Comparison of Measured and Predicted Total Rutting Resulting from Global Calibration Process. . . . .	46
Figure 5-3.	Comparison of Cumulative Fatigue Damage and Alligator Cracking Resulting from Global Calibration Process. . . . .	49
Figure 5-4.	Comparison of Measured and Predicted Lengths of Longitudinal Cracking (Top-Down Cracking) Resulting from Global Calibration Process . . . . .	50
Figure 5-5.	Comparison of Measured and Predicted Transverse Cracking Resulting from Global Calibration Process. . . . .	53
Figure 5-6.	Response Mechanisms Used in Reflection Cracking Prediction Methodology . . . . .	55
Figure 5-7.	Mechanisms of Thermally Induced Reflective Cracks of AC Overlays . . . . .	55
Figure 5-8.	Mechanisms of Traffic Induced Reflective Cracks of AC Overlays . . . . .	56
Figure 5-9.	Comparison of Measured and Predicted IRI Values Resulting from Global Calibration Process of Flexible Pavements and AC Overlays of Flexible Pavements . . . . .	62

Figure 5-10.	Comparison of Measured and Predicted IRI Values Resulting from Global Calibration Process of AC Overlays of PCC Pavements and Semi-Rigid Pavements . . . . .	62
Figure 5-11.	Comparison of Measured and Predicted Percentage JPCP Slabs Cracked Resulting from Global Calibration Process . . . . .	65
Figure 5-12.	Comparison of Measured and Predicted Transverse Cracking of Unbounded JPCP Overlays Resulting from Global Calibration Process . . . . .	65
Figure 5-13.	Comparison of Measured and Predicted Transverse Cracking for Restored JPCP Resulting from Global Calibration Process . . . . .	66
Figure 5-14.	Comparison of Measured and Predicted Transverse Joint Faulting for New JPCP Resulting from Global Calibration Process . . . . .	72
Figure 5-15.	Comparison of Measured and Predicted Transverse Joint Faulting for Unbound JPCP Overlays Resulting from Global Calibration Process . . . . .	73
Figure 5-16.	Comparison of Measured and Predicted Transverse Joint Faulting for Restored (Diamond Grinding) JPCP Resulting from Global Calibration Process . . . . .	73
Figure 5-17.	Comparison of Measured and Predicted Punchouts for New CRCP Resulting from Global Calibration Process . . . . .	77
Figure 5-18.	Illustration of Proper Location of Longitudinal Joints to Avoid Overlap with Truck Wheel Paths (to Avoid Corner Cracking) and the Resulting Critical Bending Stresses at Bottom of Slab That Are Considered to Limit Longitudinal Fatigue Cracking . . . . .	78
Figure 5-19.	Measured Longitudinal Fatigue Cracking (LCRK) versus PCC Fatigue Damage (DIF) at Bottom of PCC Slab . . . . .	79
Figure 5-20.	Comparison of Measured and Predicted Percentage SJPCP Overlay Slabs Longitudinally Cracked Resulting from Global Calibration Process . . . . .	80
Figure 5-21.	Comparison of Measured and Predicted IRI Values for New JPCP Resulting from Global Calibration Process . . . . .	82
Figure 5-22.	Comparison of Measured and Predicted IRI Values for New CRCP Resulting from Global Calibration Process . . . . .	83
Figure 7-1.	Design Reliability Concept for Smoothness (IRI) . . . . .	89
Figure 8-1.	Comparison of the Five NALS Defaults for Vehicle Class 9 Tandem Axles—Entire Range of Axle Loads . . . . .	98
Figure 8-2.	Comparison of the Five NALS Defaults for Vehicle Class 9 Tandem Axles—Axle Loads between 32,000–50,000 lb . . . . .	98
Figure 9-1.	Steps and Activities for Assessing Condition of Existing Pavements for Rehabilitation Design (Refer to Table 9-2) . . . . .	114

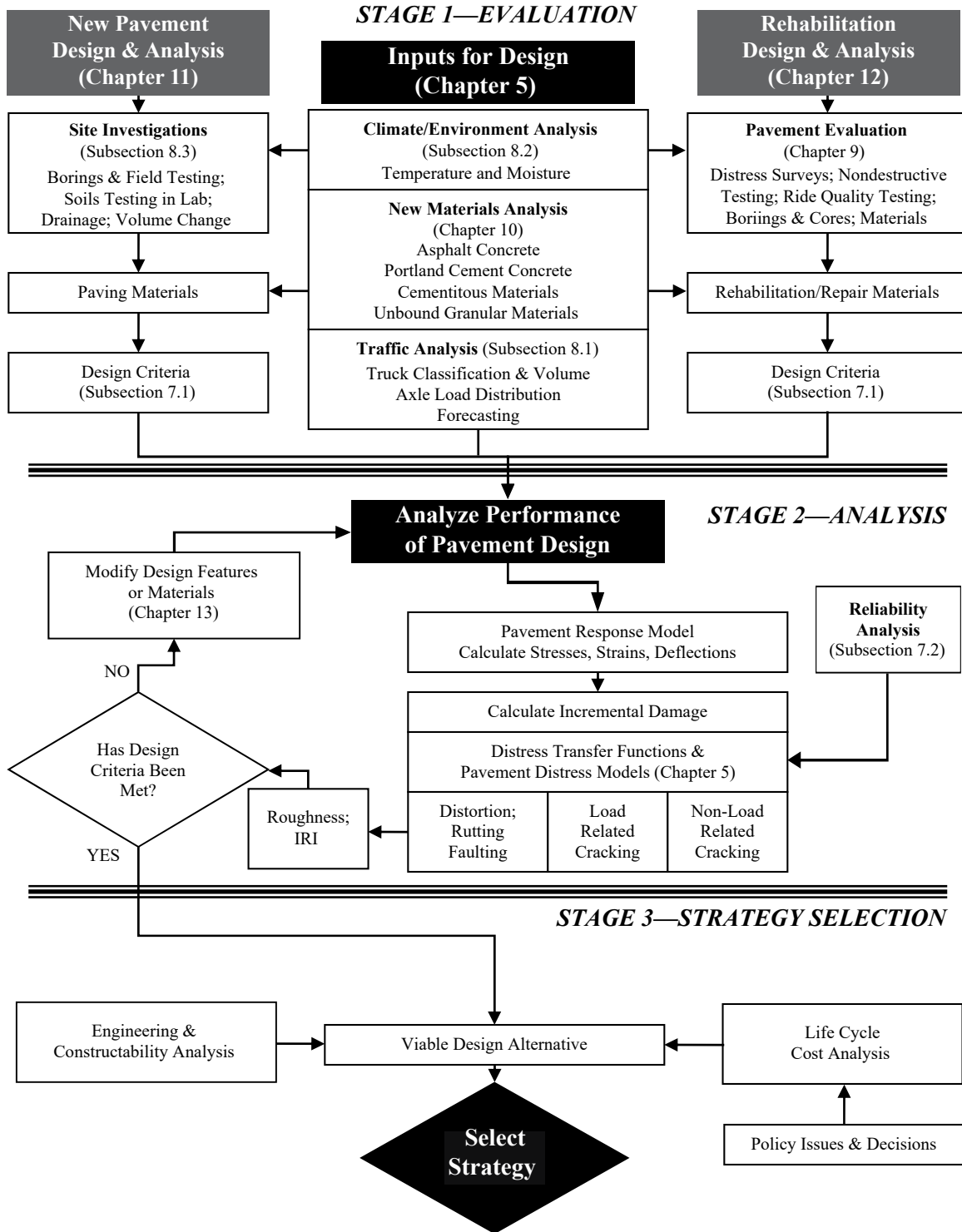


Figure 1-1. Conceptual Flow Chart of the Three-Stage Design/Analysis Process for AASHTOWare PMED

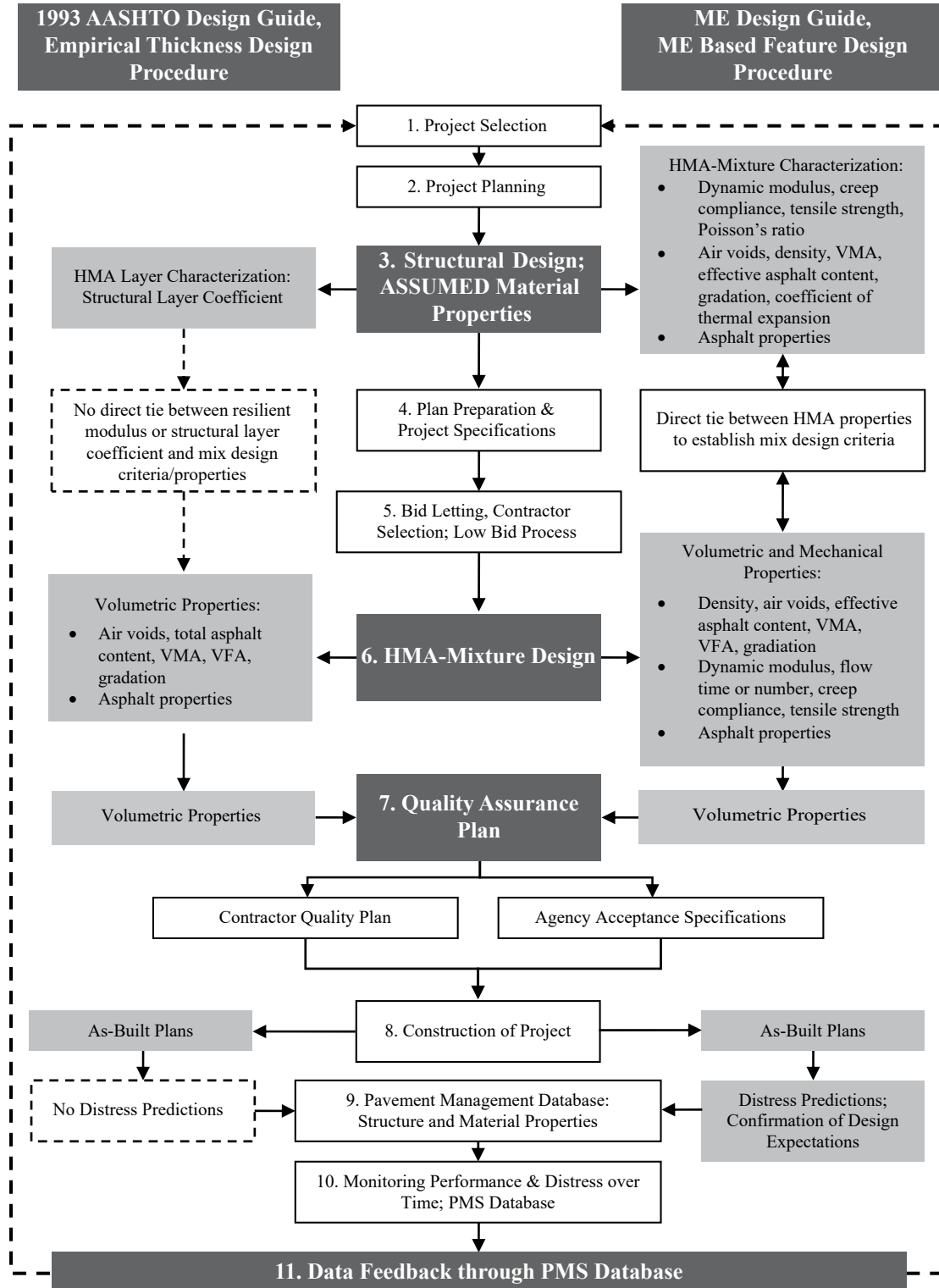


Figure 1-2. Typical Differences between Empirical Design Procedures and an Integrated ME Design System, in Terms of AC Mixture Characterization

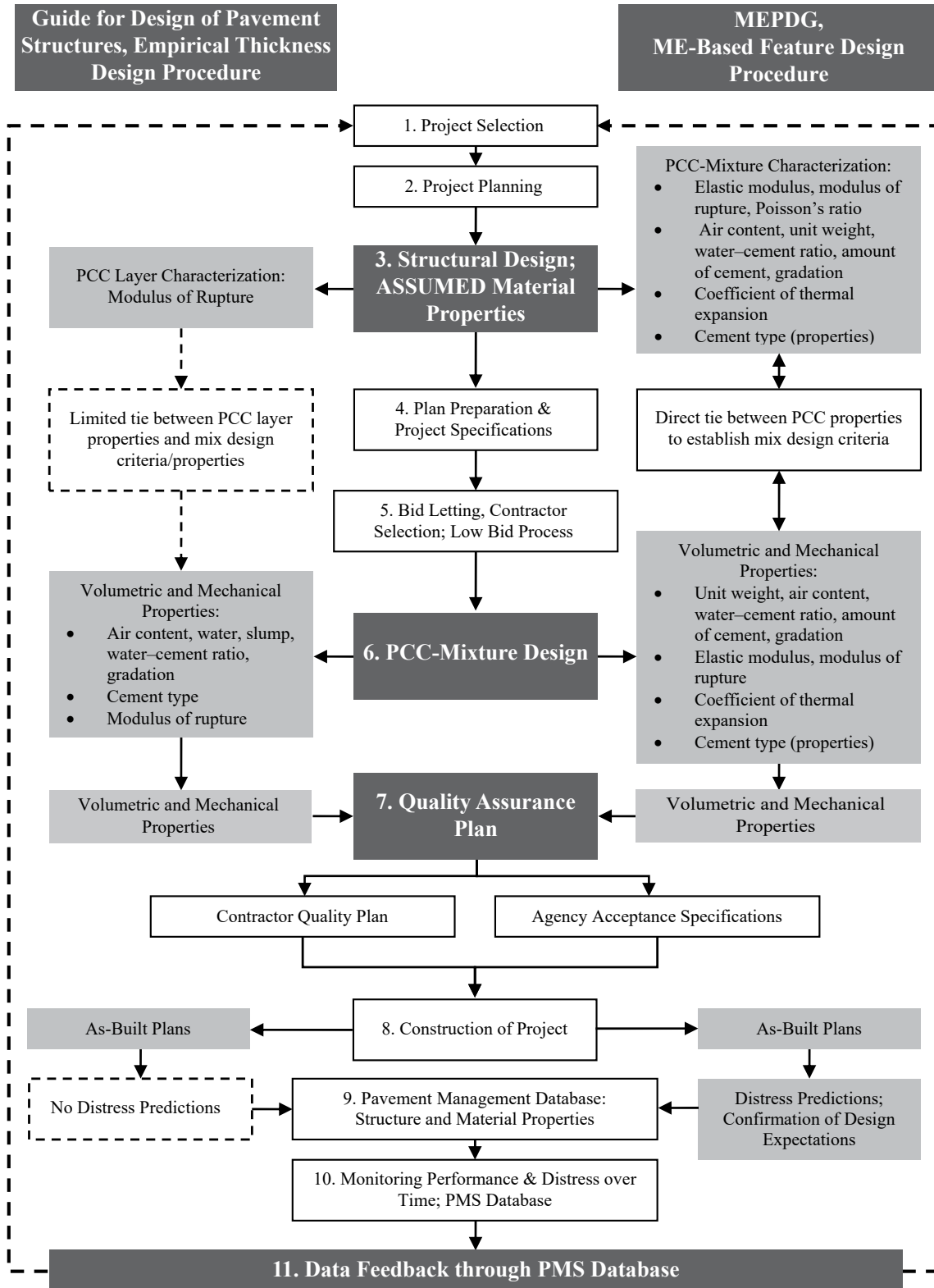


Figure 1-3. Typical Differences between Empirical Design Procedures and an Integrated ME Design System, in Terms of PCC-Mixture Characterization

The ME approach makes it possible to optimize the design and to fully verify that specific distress types will be limited to values less than the failure criteria within the design life of the pavement structure. The basic steps included in the MEPDG are listed below and presented as flow charts in Figures 1-4 and 1-5. The steps shown in Figures 1-4 and 1-5 are referenced to the appropriate sections within this manual of practice.

1. **Select a trial design strategy.** The pavement designer may use an agency-specific procedure to determine the trial design cross section.
2. **Select the appropriate performance indicator criteria (threshold value) and design reliability level for the project.** Design or performance indicator criteria include magnitudes of key pavement distresses and smoothness that may trigger major rehabilitation or reconstruction. These criteria could be a part of an agency’s policies for deciding when to rehabilitate or reconstruct. AASHTOWare PMED allows the user to select the performance indicator criteria to be considered. The user can uncheck the box next to the criteria that do not need to be considered. (See Chapter 4.1 for definitions.)
3. **Obtain all inputs for the pavement trial design under consideration.** This step may be a time-consuming effort, but it is what separates the MEPDG from other design procedures. The MEPDG allows the designer to determine inputs using a hierarchical structure in which the effort to quantify a given input is selected based on the importance of the project, importance of the input, and available resources. The required inputs to run the software are obtained using one of three levels of effort that need not be consistent for all of the inputs for a given design. This permits the user to use the “best available” data for all inputs. The hierarchical input levels are defined in Chapters 4 and 5, and are grouped under six broad topics: (1) general project information, (2) design criteria, (3) traffic, (4) climate, (5) structure layering, and (6) material properties (including the design features). *A caution to the designer—Some of the input parameters are interrelated; changing one parameter may affect the value of another input parameter. The designer should use caution in making changes in individual parameters.*
4. **Run AASHTOWare PMED and examine the inputs and outputs for engineering reasonableness.** The software calculates changes in layer properties, damage, key distresses, and the International Roughness Index (IRI) over the design life. The substeps for step 4 include:
  - a. Examine the input summary to verify the inputs are correct. This step should be completed after each run, until the designer becomes more familiar with the program and its inputs.
  - b. Examine the outputs that comprise the intermediate process—specific parameters (such as climate values), monthly load transfer efficiency (LTE) values for rigid pavement analysis, monthly layer modulus values for flexible and rigid pavement analysis to determine their reasonableness, and calculated performance indicators (pavement distresses and IRI). This step may be completed after each run or

until the designer becomes more familiar with the program. Review of important intermediate processes and steps is presented in Chapter 13.

- c. Assess whether the trial design has met each of the performance indicator criteria at the design reliability level chosen for the project. As noted above, IRI is an output parameter predicted over time and a measure of surface smoothness. IRI is calculated from other distress predictions (refer to Figure 1-1), site factors, and initial IRI.
- d. If any of the criteria are not met, determine how this deficiency can be remedied by altering the materials used, the layering of materials, layer thickness, or other design features.

5. **Revise the trial design, as needed.** If the trial design has input errors, material output anomalies, or has exceeded the failure criteria at the given level of reliability, revise the inputs/trial design and rerun the program. An automated process to iterate to an optimized thickness is done by AASHTOWare PMED to produce a feasible design.

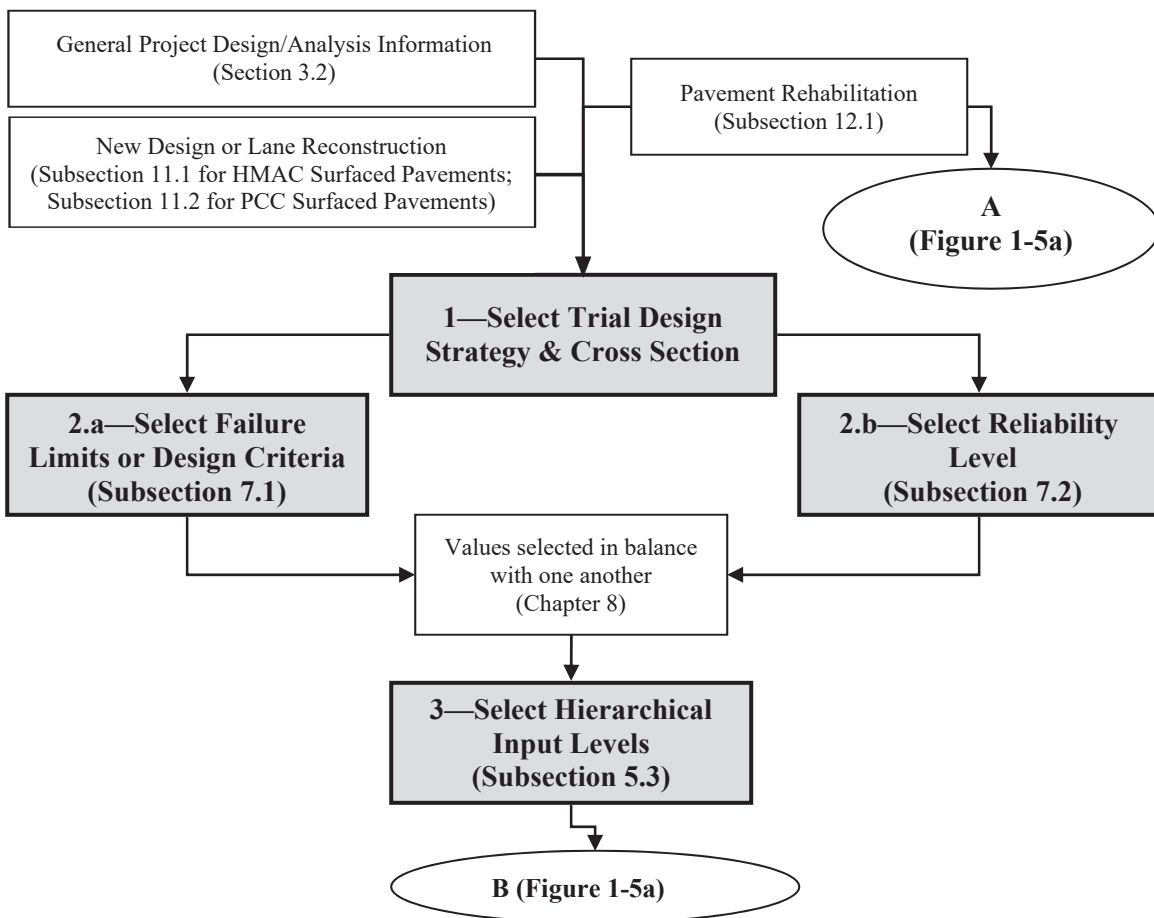


**Figure 1-4.** Flow Chart of the Steps That Are More Policy Decision Related and Needed to Complete an Analysis of a Trial Design Strategy

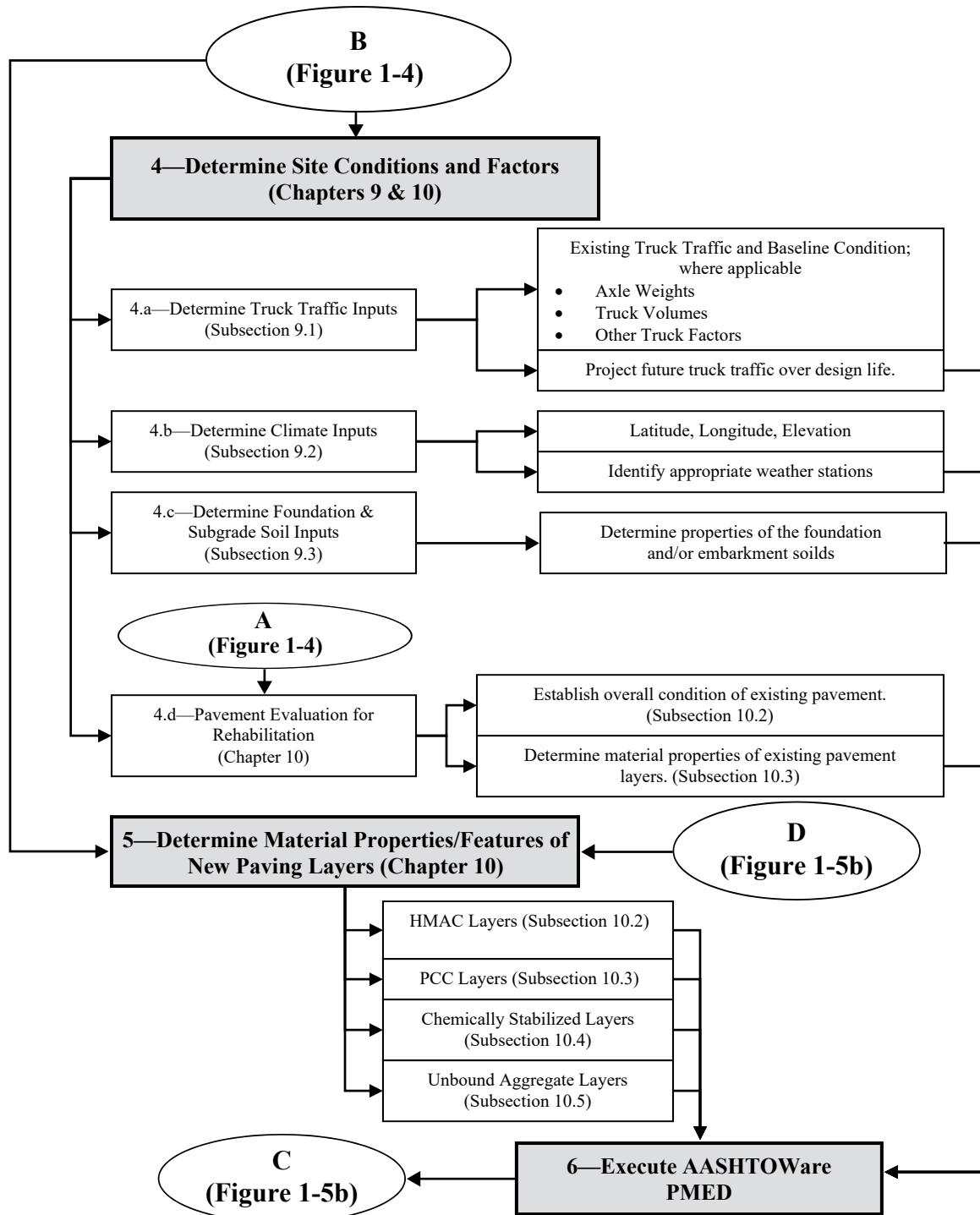


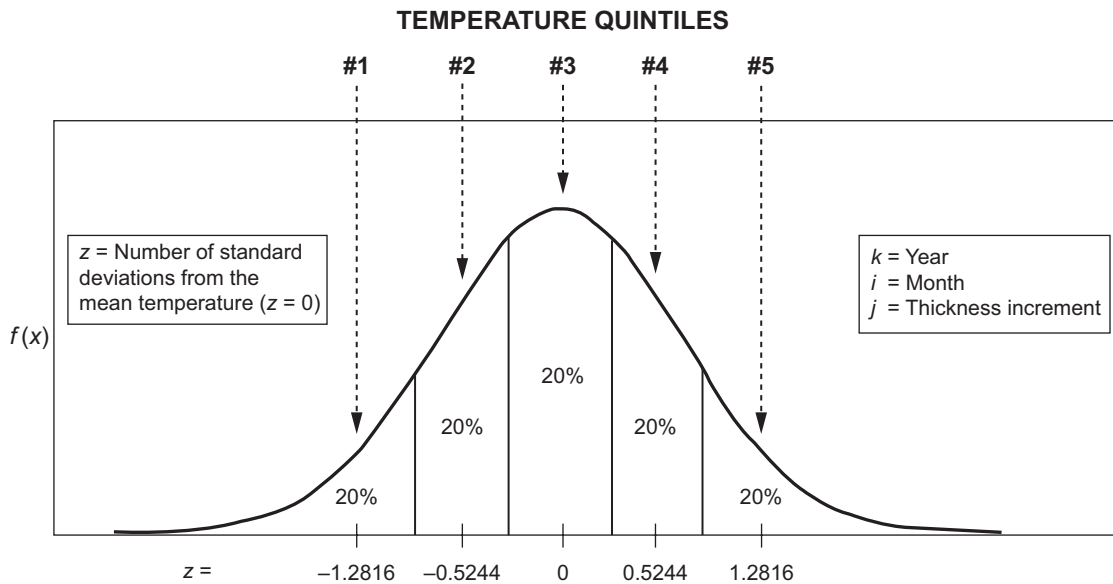
Figure 1-5a. Flow Chart of the Steps Needed to Complete an Analysis of a Trial Design Strategy

**Table 5-1.** Typical Input Levels Used in the Global Calibration of the AASHTOWare PMED Models and Transfer Functions

Input Group		Input Parameter	Recalibration Input Level Used
Truck Traffic		Axle load distributions (single, tandem, tridem)	Level 1
		Truck volume distribution	Level 1
		Lane and directional truck distributions	Level 1
		Tire pressure	Level 3, default
		Axle configuration, tire spacing	Level 3, default
		Truck wander	Level 3, default
Climate		Temperature, wind speed, cloud cover, precipitation, relative humidity	Level 1 weather stations
Material Properties	Unbound Layers and Subgrade	Resilient modulus—all unbound layers	Level 1; backcalculation
		Classification and volumetric properties	Level 1
		Moisture-density relationships	Level 1
		Soil-water characteristic relationships	Level 3, defaults
		Saturated hydraulic conductivity	Level 3, defaults
	AC	AC dynamic modulus	Level 3, defaults
		AC creep compliance and indirect tensile strength	Levels 1, 2, and 3
		Volumetric properties	Level 1
		AC coefficient of thermal expansion	Level 3, default
	PCC	PCC elastic modulus	Level 1
		PCC flexural strength	Level 1
		PCC indirect tensile strength (CRCP only)	Level 2
		PCC coefficient of thermal expansion	Level 1
All Materials		Unit weight	Level 1
		Poisson's ratio	Level 3, default
		Other thermal properties—conductivity, heat capacity, surface absorptivity	Level 3, defaults
Existing Pavement		Condition of existing layers	Levels 1 and 2

makes extensive use of the EICM for adjusting the pavement layer modulus values with temperature and moisture. The EICM calculates the temperature and moisture conditions throughout the pavement structure on an hourly basis (16).

The frequency distribution of AC temperatures using the EICM is assumed to be normally distributed. The temperatures in each AC sublayer are combined into five quintiles. Each quintile represents 20 percent of the frequency distribution for each month of the analysis period for the load related distresses (see Figure 5-1). This is accomplished by computing pavement temperatures corresponding to accumulated frequencies of 10, 30, 50, 70 and 90 percent within a given month. The average temperature within each quintile of a sublayer for each month is used to determine the dynamic modulus of that sublayer. The truck traffic is assumed to be equal within each of the five temperature quintiles. Thus, the flexible pavement procedure does not tie the hourly truck volumes directly to the hourly temperatures.



Pavement temperatures within each thickness increment of the AC layers are calculated for each month via the ICM. The pavement temperatures are then combined into five equal groups, as shown above, assuming a normal distribution. The mean pavement temperature within each group for each month for the AC thickness increment is determined for calculating the dynamic modulus as a function of time and depth in the pavement.

**Figure 5-1.** Graphical Illustration of the Five Temperature Quintiles Used in the MEPDG to Determine AC Mixture Properties for Load Related Distresses

The dynamic modulus is used to compute the horizontal and vertical strains at critical depths on a grid to determine the maximum permanent deformation within each layer and location of the maximum fatigue damage in the asphalt concrete layers. For transverse cracks (non-load related cracks), the EICM calculates the AC temperatures on an hourly basis and uses those hourly temperatures to estimate the AC properties (creep compliance and indirect tensile strength) to calculate the tensile stress throughout the AC surface layer.

The EICM also calculates the temperatures within each unbound sublayer and determines the months when any sublayer is frozen. The resilient modulus of the frozen sublayers is then increased

$$\rho = 10^9 \left\{ \frac{C_o}{\left[ 1 - (10^9)^\beta \right]} \right\}^{\frac{1}{\beta}} \quad (5-2c)$$

$$C_o = Ln \left( \frac{a_1 M_r^{b_1}}{a_9 M_r^{b_9}} \right) \quad (5-2d)$$

where:

$W_c$  = Water content, %

$M_r$  = Resilient modulus of the unbound layer or sublayer, psi

$a_{1,9}$  = Regression constants;  $a_1 = 0.15$  and  $a_9 = 20.0$

$b_{1,9}$  = Regression constants;  $b_1 = 0.0$  and  $b_9 = 0.0$

Figure 5-2 shows a comparison between the measured and predicted total rut depths, including the statistics from the global calibration process. The standard error ( $s_e$ ) for the total rut depth is the sum of the standard error for the AC and unbound layer rut depths and is a function of the average predicted rut depth. Equations 5-3a–5-3c show the standard error (standard deviation of the residual errors) for the individual layers—AC and unbound layers for coarse and fine-grained materials and soils.

$$s_{e(AC)} = 0.24(\Delta_{AC})^{0.8026} + 0.001 \quad (5-3a)$$

$$s_{e(AggrBase)} = 0.1235(\Delta_{AggrBase})^{0.5012} + 0.001 \quad (5-3b)$$

$$s_{e(Subgrade)} = 0.1477(\Delta_{Subgrade})^{0.6711} + 0.001 \quad (5-3c)$$

where:

$\Delta_{AC}$  = Plastic deformation in the AC layers, in.

$\Delta_{AggrBase}$  = Plastic deformation in the aggregate or granular base layers, in.

$\Delta_{Subgrade}$  = Plastic deformation in the subgrade or embankment layers and soils, in.

These equations for the standard errors of the predicted rut depths within each layer were not based on actual measurements of rutting within each layer, because trenches were unavailable for all LTPP test sections used in the global calibration process. The so-called “measured” rut depths within each layer were only estimated by proportioning the total rut depth measured to the different layers using a systematic procedure.

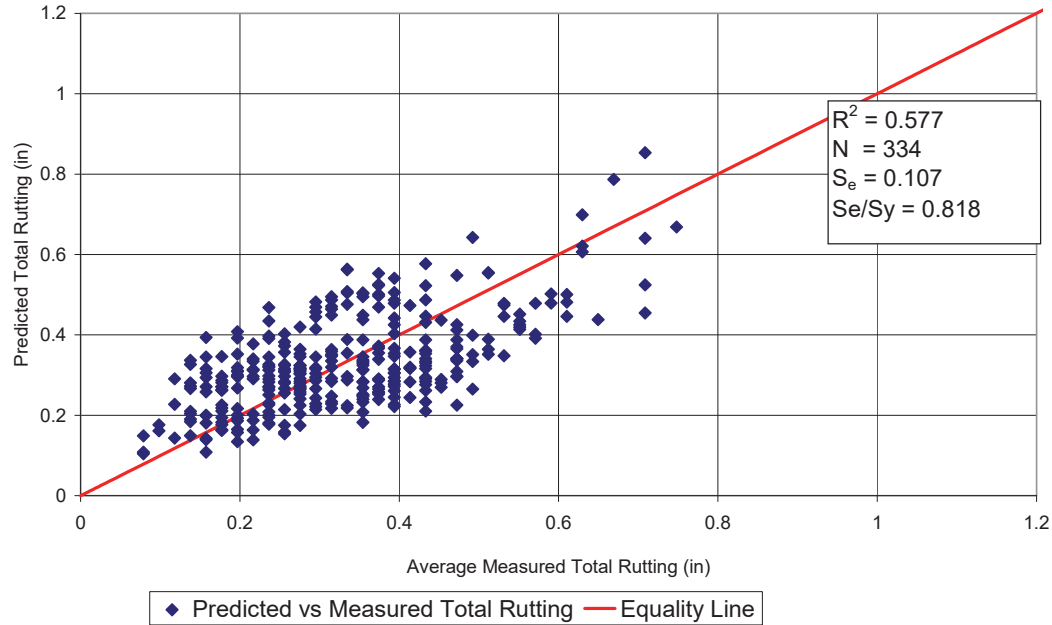


**Figure 5-2.** Comparison of Measured and Predicted Total Rutting Resulting from Global Calibration Process

### 5.3.3 Load-Related Cracking

#### Asphalt Concrete Layers

Two types of load-related cracks are predicted by the MEPDG: alligator cracking and longitudinal cracking. The MEPDG assumes that alligator, or area cracks, initiate at the bottom of the AC layers and propagate to the surface with continued truck traffic, while longitudinal cracks are assumed to initiate at the surface.

*For bottom-up or alligator cracking:*

The allowable number of axle load applications needed for the incremental damage index approach to predict bottom-up cracks) is shown in Equation 5-4a.

$$N_{f-AC} = k_{f1}(C)(C_H)\beta_{f1}(\epsilon_t)^{-k_{f2}\beta_{f2}}(E_{AC})^{-k_{f3}\beta_{f3}} \tag{5-4a}$$

where:

$N_{f-AC}$  = Allowable number of axle load applications for a flexible pavement and AC overlays

$\epsilon_t$  = Tensile strain at critical locations and calculated by the structural response model, in/in.

$E_{AC}$  = Dynamic modulus of the AC measured in compression, psi

$k_{f1}, k_{f2}, k_{f3}$  = Global laboratory-derived model coefficients for dense-graded neat AC mixtures

( $k_{f1} = 3.75, k_{f2} = 2.87, \text{ and } k_{f3} = 1.46$ )

$\beta_{f1}, \beta_{f2}, \beta_{f3}$  = Local or mixture specific field shift or adjustment constants; for the global calibration effort, these constants are:  $\beta_{f1}$  is AC thickness dependent,  $\beta_{f2}$  is 1.38, and  $\beta_{f3}$  is 0.88

For AC thicknesses less than 5 in.:  $\beta_{f1} = 0.02054$   
 For AC thicknesses 5–12 in.:  $\beta_{f1} = 5.014(H_{AC})^{-3.416}$  (5-4b)  
 For AC thicknesses greater than 12 in.:  $\beta_{f1} = 0.001032$ .

$$C = 10^M \quad (5-4c)$$

$$M = 4.84 \left( \frac{V_{be}}{V_a + V_{be}} - 0.69 \right) \quad (5-4d)$$

where:

$H_{AC}$  = Total thickness of the AC layers, in.

$V_{be}$  = Effective asphalt content by volume, %

$V_a$  = Percent air voids in the AC mixture

$C_H$  = Thickness correction term

$C_H =$	if $H_{AC} \leq 2.5$ in.	$1 / (0.005169H_{AC}^{2.913059})$
	if $2.5 \text{ in} < H_{AC} < 14.5$ in.	$1 / (-0.046908 H_{AC}^3 + 0.729644 H_{AC}^2 - 0.635578 H_{AC} - 1.555892)$
	if $H_{AC} \geq 14.5$ in.	4.255

The MEPDG calculates the incremental damage indices on a grid pattern throughout the AC layers at critical depths. The incremental damage index ( $\Delta DI$ ) is calculated by dividing the actual number of axle loads by the allowable number of axle loads (defined by Equation 5-4a, and referred to as Miner's hypothesis) within a specific time increment and axle load interval for each axle type. The cumulative damage index ( $DI$ ) for each critical location is determined by summing the incremental damage indices over time, as shown in Equation 5-5.

$$DI = \sum (\Delta DI)_{j,m,l,p,T} = \sum \left( \frac{n}{N_{f-HMA}} \right)_{j,m,l,p,T} \quad (5-5)$$

where:

$n$  = Actual number of axle load applications within a specific time period

$j$  = Axle load interval

$m$  = Axle load type (single, tandem, tridem, or quad)

$l$  = Truck type using the truck classification groups included in AASHTOWare Pavement ME Design

$p$  = Month

$T$  = Median temperature for the five temperature intervals or quintiles used to subdivide each month, °F

As noted under Subsection 4.1, General Terms, an endurance limit for AC mixtures can be input into the AASHTOWare PMED, but this concept was excluded from the global calibration process. If the endurance limit concept is selected for use, all tensile strains that are less than the endurance limit input are excluded from calculating the incremental damage index for bottom-up or alligator cracking. The endurance limit concept is not applied in calculating the incremental damage for top-down or longitudinal cracking.

The area of alligator cracking is calculated from the total damage over time (Equation 5-5) using different transfer functions. Equation 5-6a is the relationship used to predict the amount of alligator cracking on an area basis,  $FC_{Bottom}$ ,

$$FC_{Bottom} = \left( \frac{1}{60} \right) \left\{ \frac{C_4}{1 + e^{[C_1 C_1^* + C_2 C_2^* \log(DI_{Bottom} * 100)]}} \right\} \quad (5-6a)$$

where:

$FC_{Bottom}$  = Area of alligator cracking that initiates at the bottom of the AC layers, % of total lane area

$DI_{Bottom}$  = Cumulative damage index at the bottom of the AC layers

$C_{1,2,4}$  = Transfer function regression constants;  $C_4 = 6,000$ ,  $C_1 = 1.00$ , and  $C_2 = 1.00$

$$C_1^* = -2C_2^* \quad (5-6b)$$

$$C_2^* = -2.40874 - 39.748(1 + H_{AC})^{-2.856} \quad (5-6c)$$

Figure 5-3 shows the comparison of the cumulative fatigue damage and measured alligator cracking, including the statistics from the global calibration process. The standard error,  $s_e$  (standard deviation of the residual errors), for the alligator cracking prediction equation is shown in Equation 5-7, and is a function of the average predicted area of alligator cracks.

$$s_{e(Alligator)} = 1.13 + \frac{13}{1 + e^{7.57 - 15.5 \log(FC_{Bottom} + 0.0001)}} \quad (5-7)$$

$\beta_{t1}$  = Regression coefficient determined through global calibration (400)

$N[z]$  = Standard normal distribution evaluated at  $[z]$

$\sigma_d$  = Standard deviation of the log of the depth of cracks in the pavement (0.769), in.

$C_d$  = Crack depth, in.

$H_{AC}$  = Thickness of AC layers, in.

Figure 5-5 includes a comparison between the measured and predicted cracking and the statistics from the global calibration process for input Levels 1 and 3. The standard error for the transverse cracking prediction equations for the three input levels is shown in Equations 5-12a–5-12f.

$$S_c (\text{Level 1; MAAT} < 57^\circ\text{F}) = 0.14(\text{TC}) + 168 \tag{5-12a}$$

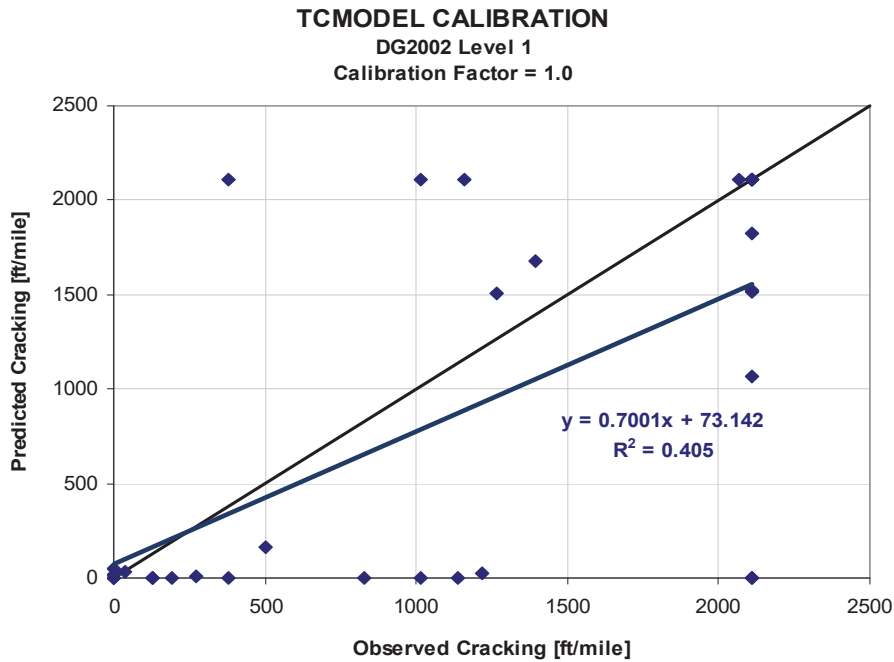
$$S_c (\text{Level 1; MAAT} > 57^\circ\text{F}) = 0.14(\text{TC}) + 343 \tag{5-12b}$$

$$S_c (\text{Level 2; MAAT} < 57^\circ\text{F}) = 0.20(\text{TC}) + 168 \tag{5-12c}$$

$$S_c (\text{Level 2; MAAT} > 57^\circ\text{F}) = 0.20(\text{TC}) + 343 \tag{5-12d}$$

$$S_c (\text{Level 3; MAAT} < 57^\circ\text{F}) = 0.289(\text{TC}) + 168 \tag{5-12e}$$

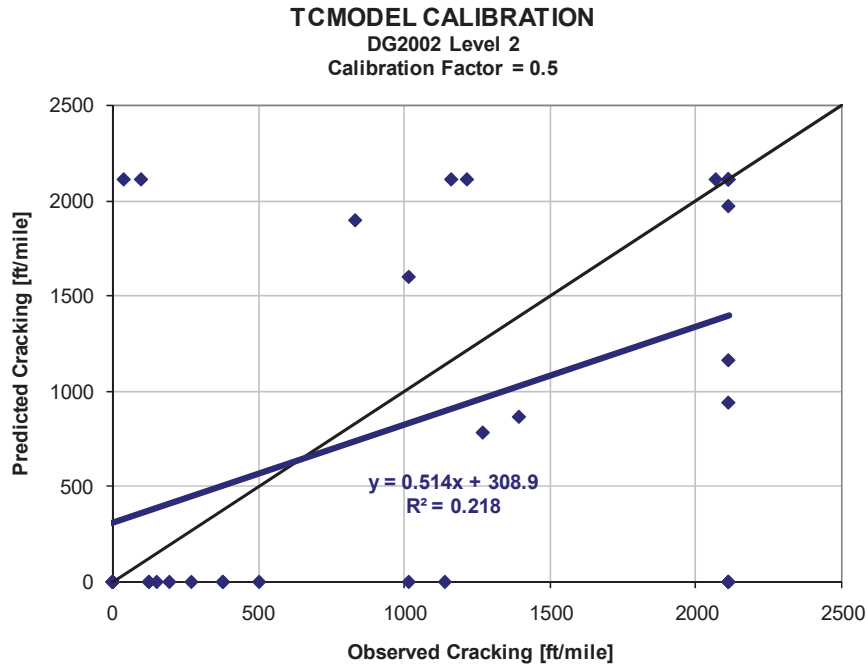
$$S_c (\text{Level 3; MAAT} > 57^\circ\text{F}) = 0.2386(\text{TC}) + 343 \tag{5-12f}$$



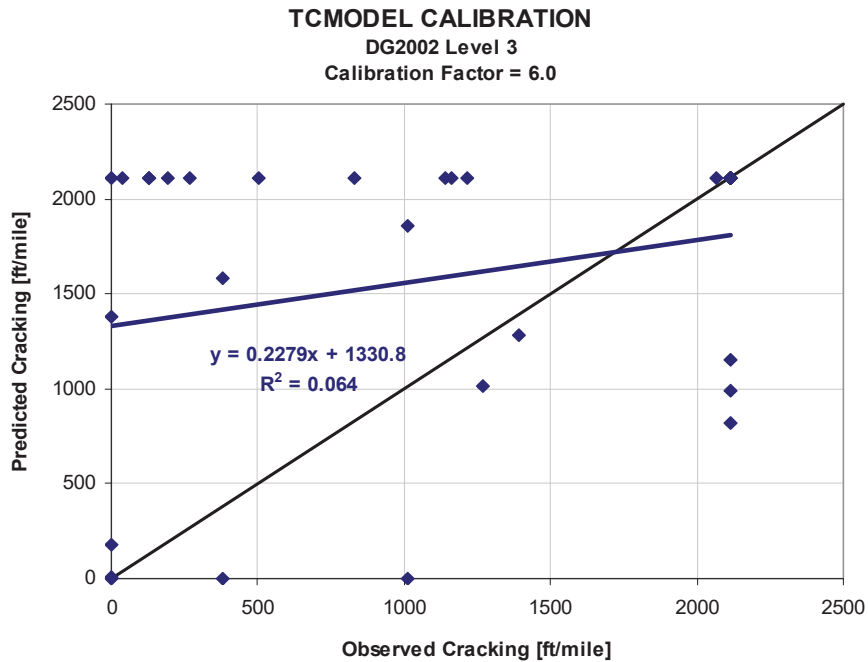
**5-5a Input Level 1 Using the Global Calibration Factor**

**Figure 5-5.** Comparison of Measured and Predicted Transverse Cracking Resulting from Global Calibration Process

*Continued on next page.*



5-5b Input Level 2 Using the Global Calibration Factor



5-5c Input Level 3 Using the Global Calibration Factor

Figure 5-5. Comparison of Measured and Predicted Transverse Cracking Resulting from Global Calibration Process, *continued*

As noted above, the  $k$ -value, or model coefficients for the reflection cracking transfer functions, are the global calibration factors and defined in Table 5-2 for transverse cracks and in Table 5-3 for fatigue cracks. The area (fatigue cracks) and length (transverse cracks) of reflection cracks from the underlying layer at month or time increment  $i$  ( $RCR_i$ ) are given by Equation 5-17.

$$RCR_i = Ckg \left( \frac{100}{c_4 + e^{c_5 \log DI_i}} \right) \quad (5-17)$$

where:

$Ckg$  = Total area or length of cracks in the existing pavement surface prior to overlay

$C_{4,5}$  = Calibration coefficients for reflection cracking

The reflective fatigue and transverse cracks are calculated separately but based on the same mathematical relationship using the appropriate calibration coefficients for fatigue and transverse cracks. The  $k$ - and  $c$ -value model coefficients are included in Table 5-2 for transverse cracks and in Table 5-3 for fatigue cracks.

**Table 5-2.** Global Calibration Coefficients for the Reflection Cracking Transfer Functions for Transverse Cracks

Calibration Coefficients	Pavement Type				
	AC over AC	AC over Intact JPCP	AC over Intact CRCP or Fractured JPCP	Semi-Rigid	AC over Semi-Rigid
$k_1$	0.012	0.012	0.012	0.45	0.012
$k_2$	0.005	0.005	0.0002	0.05	0.005
$k_3$	1.00	1.00	0.1	1.0	1.0
$C_1$	3.22	3.22	3.22	0.1	3.22
$C_2$	25.7	25.7	25.7	0.9809	25.7
$C_3$	0.1	0.1	0.1	0.19	0.1
$C_4$	133.4	133.4	133.4	165.3	133.4
$C_5$	-72.4	-72.4	-72.4	-5.1048	-72.4

**Table 5-3.** Global Calibration Coefficients for the Reflection Cracking Transfer Functions for Fatigue Cracks

Calibration Coefficients	Pavement Type				
	AC over AC	AC over Intact JPCP	AC over Intact CRCP or Fractured JPCP	Semi-Rigid	AC over Semi-Rigid
$k_1$	0.012	NA	NA	0.45	0.012
$k_2$	0.005	NA	NA	0.05	0.005
$k_3$	1.00	NA	NA	1.00	1.00
$C_1$	0.38	NA	NA	1.64	0.38
$C_2$	1.66	NA	NA	1.1	1.66
$C_3$	2.72	NA	NA	0.19	2.72
$C_4$	105.4	NA	NA	62.1	105.4
$C_5$	-7.02	NA	NAA	-404.6	-7.02

For each month,  $i$ , there will be an increment of damage,  $\Delta DI_i$ , which will cause an increment of cracking area and/or length,  $CA_i$ , to the wearing surface or overlay. To estimate the amount of cracking reflected from the non-surface layer to the surface of the pavement for month  $m$ , the reflective cracking prediction equation is applied incrementally. The standard deviation equations for the standard error are listed in Table 5-4 for transverse cracks and in Table 5-5 for fatigue cracks.

**Table 5-4.** Standard Deviation Equations for the Transverse Cracks

Pavement Type	Standard Deviation Equation
AC over AC	$70.98(TC)^{0.2994} + 30.12$
AC over Intact JPCP	$5.1025(TC)^{0.6513} + 30.12$
AC over Intact CRCP or Fractured JPCP	$52.54(TC)^{0.39} + 283.3$
Semi-Rigid	$0.000027(TC)^{2.1187} + 399.9$
AC over Semi-Rigid	$70.98(TC)^{0.2994} + 30.12$

Note:  $TC$  = Total length of predicted transverse cracks in ft/mi

**Table 5-5.** Standard Deviation Equations for the Fatigue Cracks

Pavement Type	Standard Deviation Equation
AC over AC	$1.1097(FC)^{0.6804} + 1.23$
AC over Intact JPCP	Not Applicable
AC over Intact CRCP or Fractured JPCP	Not Applicable
Semi-Rigid	$1.3897(FC)^{0.2960} + 0.4212$
AC over Semi-Rigid	$1.1097(FC)^{0.6804} + 1.23$

Note:  $FC$  = Total area of predicted bottom-up fatigue or alligator cracks in percent total lane area.

## 5.4 Distress Prediction Equations for Rigid Pavements and PCC Overlays

The following summarizes the methodology and mathematical models used to predict each rigid pavement and PCC overlay performance indicator. The PCC model coefficients were based on the results and findings from NCHRP 20-07, Task 327, and are included in the following sections.

### 5.4.1 Transverse Slab Cracking (Bottom-Up and Top-Down)—JPCP

As stated earlier for JPCP transverse cracking, both bottom-up and top-down modes of cracking are considered. Under typical service conditions, the potential for either mode of cracking is present in all slabs. Any given slab cracks either from bottom-up or top-down, but not both. Therefore, the predicted bottom-up and top-down cracking are not particularly meaningful by themselves, and combined cracking is reported excluding the possibility of both modes of cracking occurring on the same slab.

The percentage of slabs with transverse cracks (including all severities) in a given traffic lane is used as the measure of transverse cracking, and is predicted using the following global equation for both bottom-up and top-down cracking:

$$CRK = \frac{100}{1 + C_4(DI_F)^{C_5}} \quad (5-19)$$

where:

$CRK$  = Predicted amount of bottom-up or top-down cracking (fraction)

$DI_F$  = Fatigue damage calculated using the procedure described in this section

$C_{4,5}$  = Calibration coefficients;  $C_4 = 0.52$ ,  $C_5 = -2.17$

The general expression for fatigue damage accumulations considering all critical factors for JPCP transverse cracking is known as Miner's hypothesis, and is calculated as follows:

$$DI_F = \sum \frac{n_{i,j,k,l,m,n,o}}{N_{i,j,k,l,m,n,o}} \quad (5-20a)$$

where:

$DI_F$  = Total fatigue damage (top-down or bottom-up)

$n_{i,j,k,\dots}$  = Applied number of load applications at condition  $i, j, k, l, m, n$

$N_{i,j,k,\dots}$  = Allowable number of load applications at condition  $i, j, k, l, m, n$

$i$  = Age (accounts for change in PCC modulus of rupture and elasticity, slab/base contact friction, and deterioration of shoulder LTE)

$j$  = Month (accounts for change in base elastic modulus and effective dynamic modulus of subgrade reaction)

$k$  = Axle type (single, tandem, and tridem for bottom-up cracking; short, medium, and long wheel-base for top-down cracking)

$l$  = Load level (incremental load for each axle type)

$m$  = Equivalent temperature difference between top and bottom PCC surfaces

$n$  = Traffic offset path

$o$  = Hourly truck traffic fraction

The applied number of load applications ( $n_{i,j,k,l,m,n}$ ) is the actual number of axle type,  $k$ , of load level,  $l$ , that passed through traffic path,  $n$ , under each condition  $i, j$ , and  $m$  (age, season, and temperature difference). The allowable number of load applications is the number of load cycles at which fatigue failure is expected (corresponding to 50 percent slab cracking) and is a function of the applied stress and PCC strength. The allowable number of load applications is determined using the following PCC fatigue equation:

$$\log(N_{i,j,k,l,m,n}) = C_1 \cdot \left( \frac{MR_i}{\sigma_{i,j,k,l,m,n}} \right)^{C_2} \quad (5-20b)$$

where:

$N_{i,j,k,l,m,n}$  = Allowable number of load applications at condition  $i, j, k, l, m, n$

$M_{Ri}$  = PCC modulus of rupture at age  $i$ , psi

$\sigma_{i,j,k,l,m,n}$  = Applied stress at condition  $i, j, k, l, m, n$

$C_1$  = Calibration constant, 2.0

$C_2$  = Calibration constant, 1.22

The fatigue damage calculation is a process of summing damage from each damage increment. Once top-down and bottom-up damage are estimated, the corresponding cracking is computed using Equation 5-19 and the total combined cracking is determined using Equation 5-21.

$$TCRACK = (CRK_{Bottom-up} + CRK_{Top-down} - CRK_{Bottom-up} \cdot CRK_{Top-down}) \cdot 100\% \quad (5-21)$$

where:

$TCRACK$  = Total transverse cracking (percent, all severities)

$CRK_{Bottom-up}$  = Predicted amount of bottom-up transverse cracking (fraction) and

$CRK_{Top-down}$  = Predicted amount of top-down transverse cracking (fraction)

It is important to note that Equation 5-21 assumes that a slab cracks from either bottom-up or top-down, but not both. A plot of measured versus predicted transverse cracking and the statistics resulting from the global calibration process is shown in Figures 5-11 through 5-13.

Calculation of critical responses using neural nets (for speed) requires that the slab and base course are combined into an equivalent section based on equivalent stresses (load and temperature/moisture gradients) and contact friction between slab and base. This is done monthly as these parameters change over time.

$$FAULTMAX_i = FAULTMAX_{i-1} + C_7 \times \frac{\sum_{j=1}^m DE_j}{10^6} \times \text{Log}(1 + C_5 \times 5.0^{EROD})^{C_6} \quad (5-23c)$$

$$FAULTMAX_0 = C_{12} \cdot \delta_{curling} \cdot \left[ \log(1 + C_5 \cdot 5.0^{EROD}) \cdot \log\left(\frac{P_{200} \cdot WetDays}{P_s}\right) \right]^{C_6} \quad (5-23d)$$

where:

$Fault_m$  = Mean joint faulting at the end of month  $m$ , in.

$\Delta Fault_i$  = Incremental change (monthly) in mean transverse joint faulting during month  $i$ , in.

$FAULTMAX_i$  = Maximum mean transverse joint faulting for month  $i$ , in.

$FAULTMAX_0$  = Initial maximum mean transverse joint faulting, in.

$DE_i$  = Differential density of energy of subgrade deformation accumulated during month  $i$  (see Equation 5-27a)

$EROD$  = Base/subbase erodibility factor

$\delta_{curling}$  = Maximum mean monthly slab corner upward deflection PCC due to temperature curling and moisture warping

$P_s$  = Overburden on subgrade, lb

$P_{200}$  = Percent subgrade material passing #200 sieve

$WetDays$  = Average annual number of wet days (greater than 0.1-in. rainfall)

$C_{1,2,3,4,5,6,7,12,34}$  = Global calibration constants ( $C_1 = 0.595$ ,  $C_2 = 1.636$ ,  $C_3 = 0.00217$ ,  $C_4 = 0.00444$ ,  $C_5 = 250$ ,  $C_6 = 0.47$ ,  $C_7 = 7.3$ ,  $C_8 = 400$ , and  $C_{12}$  and  $C_{34}$  are defined by Equations 5-23e and 5-25f). Constants used for restored rigid pavements are:  $C_1 = 0.6$ ,  $C_2 = 1.2$ ,  $C_3 = 0.002125$ ,  $C_4 = 0.000884$ ,  $C_5 = 400$ ,  $C_6 = 0.4$ , and  $C_7 = 1.83312$ )

$$C_{12} = C_1 + C_2 \cdot FR^{0.25} \quad (5-23e)$$

$$C_{34} = C_3 + C_4 \cdot FR^{0.25} \quad (5-23f)$$

$FR$  = Base freezing index defined as percentage of time the top base temperature is below freezing (32°F) temperature

For faulting analysis, each passing of an axle causes only one occurrence of critical loading, that is, when DE has the maximum value. Since the maximum faulting development occurs during nighttime when the slab is curled upward, joints are opened, and the load transfer efficiencies are lower, only axle load repetitions applied from 8:00 p.m. to 8:00 a.m. are considered in the faulting analysis.

For faulting analysis, the equivalent linear temperature difference for nighttime is determined for each calendar month as the mean difference between top and bottom PCC surfaces occurring from 8:00 p.m. to 8:00 a.m. The equivalent temperature gradient for each month of the year is then determined as follows:

$$\Delta T_m = \Delta T_{t,m} - \Delta T_{b,m} + \Delta T_{sh,m} + \Delta T_{PCW} \quad (5-24)$$

where:

$\Delta T_m$  = Effective temperature differential for month  $m$

$\Delta T_{t,m}$  = Mean PCC top-surface nighttime temperature (from 8:00 p.m. to 8:00 a.m.) for month  $m$

$\Delta T_{b,m}$  = Mean PCC bottom-surface nighttime temperature (from 8:00 p.m. to 8:00 a.m.) for month  $m$

$\Delta T_{sh,m}$  = For old concrete, equivalent temperature differential due to reversible shrinkage for month  $m$  (i.e., shrinkage is fully developed)

$\Delta T_{PCW}$  = Equivalent temperature differential due permanent curl/warp

The temperature in the top PCC layer is computed at 11 evenly spaced points through the thickness of the PCC layer at every hour using the available climatic data. These temperature distributions are converted into the equivalent difference of temperatures between the top and bottom PCC surfaces.

The corner deflections due to slab curling and shrinkage warping are determined each month using the effective temperature differential for each calendar month, corresponding effective  $k$ -value, and base modulus for the month. The corner deflections are determined using a finite, element-based, neural network, rapid response solution methodology implemented in the AASHTOWare PMED software. The initial maximum faulting is determined using the calculated corner deflections and Equation 5-23d.

Using Equation 5-23c, the maximum faulting is adjusted for the past traffic damage using past cumulative differential energy (i.e., differential energy accumulated from axle-load applications for all months prior to the current month). For each increment and each axle type and axle-load, deflections at the loaded and unloaded corner of the slab are calculated using the neural networks.

The magnitudes of corner deflections of loaded and unloaded slabs are highly affected by the joint LTE. The LTE from aggregate interlock, dowels (if present), and base/subgrade are determined in order to evaluate initial transverse joint LTE. Table 5-8 lists the  $LTE_{base}$  values that are included in the AASHTOWare PMED software. The  $LTE_{agg}$  and  $LTE_{dowel}$  values are explained in latter paragraphs of this section. After the contributions of the aggregate interlock, dowels, and base/subgrade are determined, the total initial joint load transfer efficiency is determined as follows:

$$LTE_{joint} = 100 \left[ 1 - (1 - LTE_{dowel} / 100)(1 - LTE_{agg} / 100)(1 - LTE_{base} / 100) \right] \quad (5-25)$$

where:

$LTE_{joint}$  = Total transverse joint LTE, %

$LTE_{dowel}$  = Joint LTE if dowels are the only mechanism of load transfer, %

$LTE_{base}$  = Joint LTE if the base is the only mechanism of load transfer, %

$LTE_{agg}$  = Joint LTE if aggregate interlock is the only mechanism of load transfer, %

The LTE is determined and output for each calendar month can be observed over time to see if it maintains a high level. If the mean nighttime PCC temperature at the mid-depth is below freezing (32°F), then joint LTE for that month is increased. That is done by assigning a 90 percent base LTE for that month. The aggregate interlock and dowel component of LTE are adjusted every month.

**Table 5-6.** Assumed Effective Base LTE for Different Base Types

Base Type	$LTE_{Base}$
Aggregate Base	20%
ATB or CTB	30%
Lean Concrete Base	40%

The  $LTE_{dowel}$  value (portion of the  $LTE_{joint}$  from the mechanism of load transfer from the dowels) is determined in accordance with Equation 5-26a.

$$LTE_{dowel} = \frac{1}{0.01 + 0.012J_d^{-0.849}} \quad (5-26a)$$

and

$$J_d = J_d^* + (J_o - J_d^*)e^{-DAM_{dowel}} \quad (5-26b)$$

where:

$J_d$  = Non-dimensional dowel stiffness at the time of load application

$J_o$  = Initial non-dimensional dowel stiffness

$J_d^*$  = Critical non-dimensional dowel stiffness

$DAM_{dowel}$  = Damage at the dowel-concrete interface

The dowel damage,  $DAM_{dowel}$  is determined as follows:

$$DAM_{dowel} = C_8 \sum_j \frac{J_d (\delta_{loaded} - \delta_{unloaded})(dsp)}{df'_c} \quad (5-26c)$$

where:

$C_8$  = Coefficient equal to 400

$\delta_{loaded}$  = Deflection at the corner of the loaded slab induced by the axle, in.

$\delta_{unloaded}$  = Deflection at the corner of the unloaded slab induced by the axle, in.

$dsp$  = Space between adjacent dowels in the wheel path, in.

$f'_c$  = PCC compressive strength, psi

$d$  = Dowel diameter, in.

Using Equation 5-23c, the maximum faulting is adjusted for the past traffic damage using past cumulative differential energy (i.e., differential energy accumulated from axle load applications for all months prior to the current month). For each increment and for each axle type and axle load,

deflections at the loaded and unloaded corner of the slab are calculated using the neural networks. Using these deflections, the differential energy of subgrade deformation,  $DE$ , shear stress at the slab corner,  $\tau$ , and (for doweled joints) maximum dowel bearing stress,  $\sigma_b$ , are calculated:

$$DE = \frac{k}{2} (\delta_{loaded}^2 - \delta_{unloaded}^2) \quad (5-27a)$$

$$\tau = \frac{dsk(dsp)(\delta_{loaded} - \delta_{unloaded})}{h_{PCC}} \quad (5-27b)$$

$$\sigma_b = \frac{\zeta_d (\delta_{loaded} - \delta_{unloaded})}{d(dsp)} \quad (5-27c)$$

$$dsk = k * l * \left[ \frac{\left( \frac{1}{LTE_{dowel}} \right) - 0.01}{0.012} \right]^{-1.1779} \quad (5-27d)$$

where:

$DE$  = Differential energy, lb/in.

$\delta_{loaded}$  = Loaded corner deflection, in.

$\delta_{unloaded}$  = Unloaded corner deflection, in.

$AGG$  = Aggregate interlock stiffness factor

$k$  = Coefficient of subgrade reaction, psi/in.

$h_{PCC}$  = PCC slab thickness, in.

$\zeta_d$  = Dowel stiffness factor =  $J_d * k * l * dsp$

$d$  = Dowel diameter, in.

$dsp$  = Dowel spacing, in.

$J_d$  = Non-dimensional dowel stiffness at the time of load application

$l$  = Radius of relative stiffness, in.

The incremental loss of shear capacity ( $\Delta s$ ) due to repeated wheel load applications within each month is characterized in terms of the width of the transverse joint. This is based on a function derived from the analysis of load transfer test data developed by the Portland Cement Association (PCA). The following loss of shear occurs during the time increment (month):

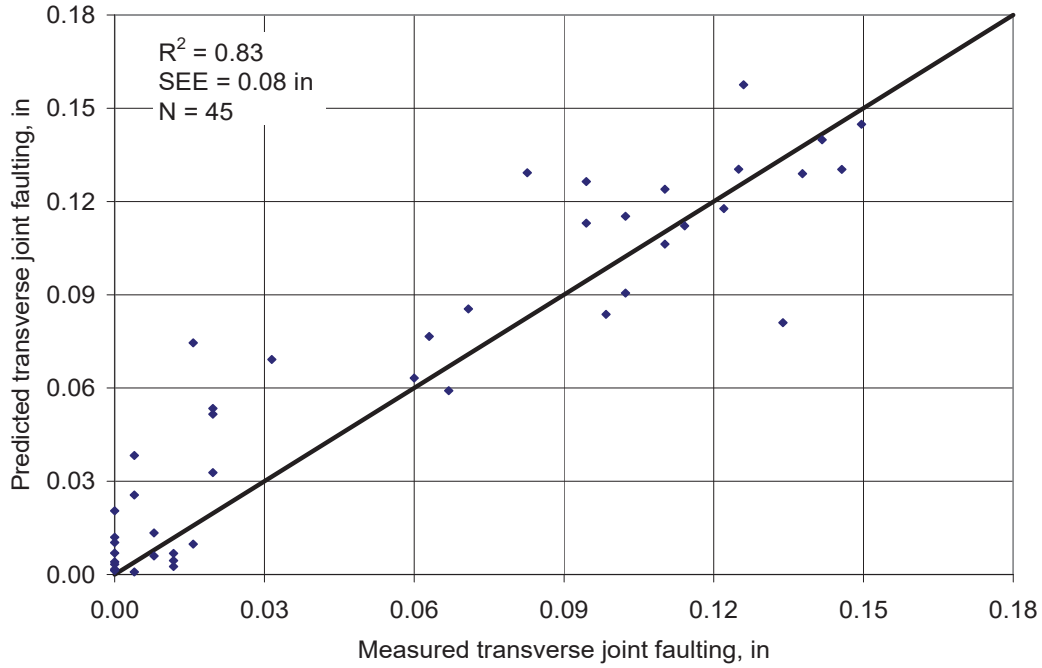


**Figure 5-15.** Comparison of Measured and Predicted Transverse Joint Faulting for Unbound JPCP Overlays Resulting from Global Calibration Process

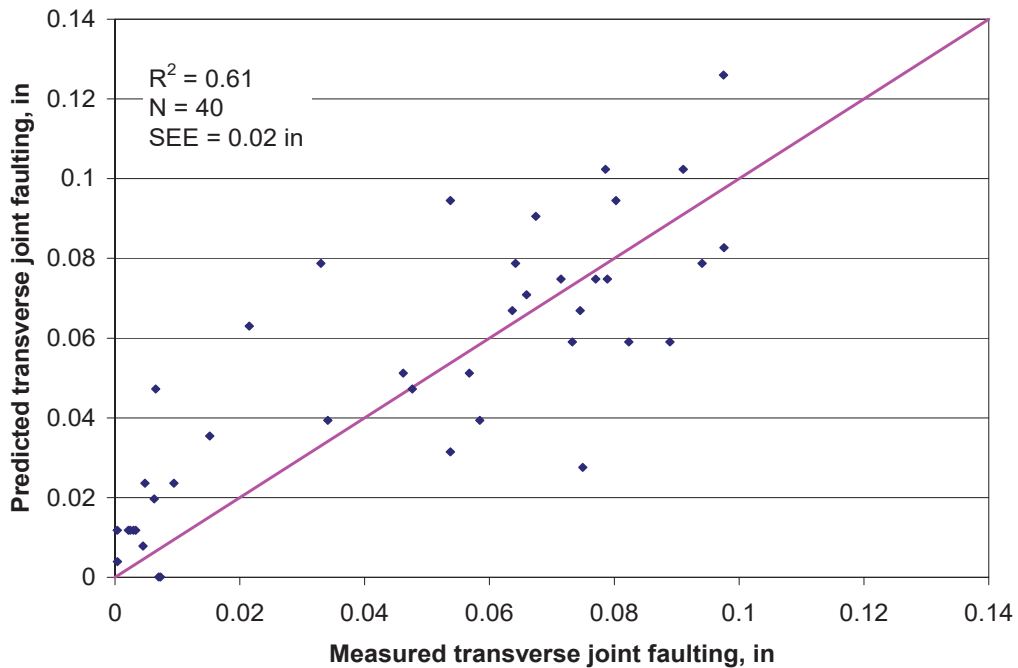


**Figure 5-16.** Comparison of Measured and Predicted Transverse Joint Faulting for Restored (Diamond Grinding) JPCP Resulting from Global Calibration Process

### 5.4.3 CRCP Punchouts

The following globally calibrated model predicts CRCP punchouts as a function of accumulated fatigue damage due to top-down stresses in the transverse direction:

$$PO = \frac{C_3}{1 + C_4 (DI_{PO})^{C_5}} \quad (5-30)$$

where:

$PO$  = Total predicted number of medium and high severity punchouts per mile

$DI_{PO}$  = Accumulated fatigue damage (due to slab bending in the transverse direction) at the end of  $y^{\text{th}}$  year

$C_3, C_4, C_5$  = Calibration constants (107.73, 2.475, and  $-0.785$ , respectively)

Subsection 11.2.3, CRCP Design, identifies the more important factors that affect the number of punchouts and crack spacing, which determine the overall performance of CRCP. The mean crack spacing for the selected trial design and time of construction is calculated in accordance with Equation 5-31.

$$\bar{L} = \frac{(f_t - \sigma_{env})}{\frac{f}{2} + \frac{U_m P_{steel}}{c_1 d_b}} \quad (5-31)$$

where:

$\bar{L}$  = Mean transverse crack spacing, in.

$f_t$  = Concrete indirect tensile strength, psi

$f$  = Base friction coefficient

$U_m$  = Peak bond stress, psi

$P_{steel}$  = Percent longitudinal steel

$d_b$  = Reinforcing steel bar diameter, in.

$c_1$  = First bond stress coefficient

$\sigma_{env}$  = Tensile stress in the PCC due to environmental curling, psi

The environmental tensile stress in the PCC from the slab curing is calculated in accordance with Equation 5-32:

$$\sigma_{env} = B_{curl} \sigma_0 \left( 1 - \frac{2D_{steel}}{h_{PCC}} \right) \quad (5-32)$$

where:

$H_{PCC}$  = Slab thickness, in.

$D_{steel}$  = Depth to steel layer, in.

$B_{curl}$  = Bradbury's curling/warping stress coefficient

$\sigma_0$  = Westergaard's nominal stress factor based on PCC modulus, Poisson's ratio, unrestrained curling, and warping strain

The damage accumulated at the critical point on top of the slab is calculated for each time increment of the design life. Damage is calculated in the following manner:

- For the given time increment, calculate crack width at the level of steel as a function of drying shrinkage, thermal contraction, and the restraint from reinforcing steel and base friction:

$$cw = \text{Max} \left[ L \left( \varepsilon_{shr} + \alpha_{PCC} \Delta T_{\zeta} - \frac{c_2 f_{\sigma long}}{E_{PCC}} \right) (C_c) 1000 \right] \quad (5-33)$$

where:

$cw$  = Average crack width at the depth of the steel, mils

$L$  = Mean crack spacing based on design crack distribution, in.

$\varepsilon_{shr}$  = Unrestrained concrete drying shrinkage at steel depth,  $\times 10^{-6}$

$\alpha_{PCC}$  = PCC coefficient of thermal expansion, /°F

$\Delta T_{\zeta}$  = Drop in PCC temperature from the concrete set temperature at the depth of the steel for construction month, °F

$c_2$  = Second bond stress coefficient

$f_{\sigma long}$  = Maximum longitudinal tensile stress in PCC at steel level, psi

$E_{PCC}$  = PCC elastic modulus, psi

$C_c$  = Local calibration constant ( $C_c = 1$  for the global calibration)

- For the given time increment, calculate shear capacity, crack stiffness, and LTE across transverse cracks. LTE is determined as:

$$LTE_{TOT} = 100 * \left\{ 1 - \left[ 1 - \frac{1}{1 + \log^{-1} \frac{0.214 - 0.183 \frac{a}{l} - \log(J_c) - r_d}{1.18}} \right] \left( 1 - \frac{LTE_{Base}}{100} \right) \right\} \quad (5-34)$$

where:

$LTE_{TOT}$  = Total crack LTE due to aggregate interlock, steel reinforcement, and base support, %

$l$  = Radius of relative stiffness computed for time increment  $i$ , in.

$a$  = Radius for a loaded area, in.

$r_d$  = Residual dowel-action factor to account for residual load transfer provided by the steel reinforcement =  $2.5P_{steel} - 1.25$

$LTE_{Base}$  = Base layer contribution to the LTE across transverse crack, % (Typical values were given in Table 5-6)

$J_c$  = Joint stiffness on the transverse crack for current time increment

$P_{steel}$  = Percent steel reinforcement

- The loss of support for the given time increment is calculated using the base erosion model. The loss of support is a function of base type, quality of base material, precipitation, and age.
- For each load level in each gear configuration or axle-load spectra, the tensile stress on top of slab is used to calculate the number of allowable load repetitions,  $N_{i,j}$ , due to this load level in this time increment as:

$$\log N_{i,j} = C_1 * \left( \frac{M_{Ri}}{\sigma_{i,j}} \right)^{C_2} - 1 \quad (5-35)$$

where:

$M_{Ri}$  = PCC modulus of rupture at age  $i$ , psi

$\sigma_{i,j}$  = Applied stress at time increment  $i$  due to load magnitude  $j$ , psi

$C_{1,2}$  = Calibration constants ( $C_1 = 2.0$  and  $C_2 = 1.22$ )

- The loss in shear capacity and loss in load transfer is calculated at the end of the time increment in order to estimate these parameters for the next time increment. The crack LTE is output monthly for evaluation. A minimum of 90–95 percent is considered good LTE over the design period.

The critical stress at the top of the slab that is transverse and located near a transverse crack was found to be 40–60 in. from the edge (48 in. was used, since this was often the critical location). A crack spacing of 2 ft was used as the critical width after observations that a very high percentage of punchouts were 2 ft or less. This stress is calculated using the neural net models, which are a function of slab thickness, traffic offset from edge, PCC properties, base course properties and thickness, subgrade stiffness, equivalent temperature gradient, and other factors.

Fatigue damage,  $FD$ , due to all wheel loads in all time increments is calculated (according to Miner’s damage hypothesis) by summing the damage over design life in accordance with Equation 5-20a. Once damage is estimated using Equation 5-20a, the corresponding punchouts are computed using the globally calibrated Equation 5-30.

A plot of measured versus predicted CRCP punchouts and statistics from the global calibration is shown in Figure 5-17. The standard error for the CRCP punchouts prediction model is shown in Equation 5-36.

$$s_{e(PO)} = 2.208(PO)^{0.5316} \quad (5-36)$$

where:

$PO$  = Predicted mean medium and high severity punchouts, no./mile

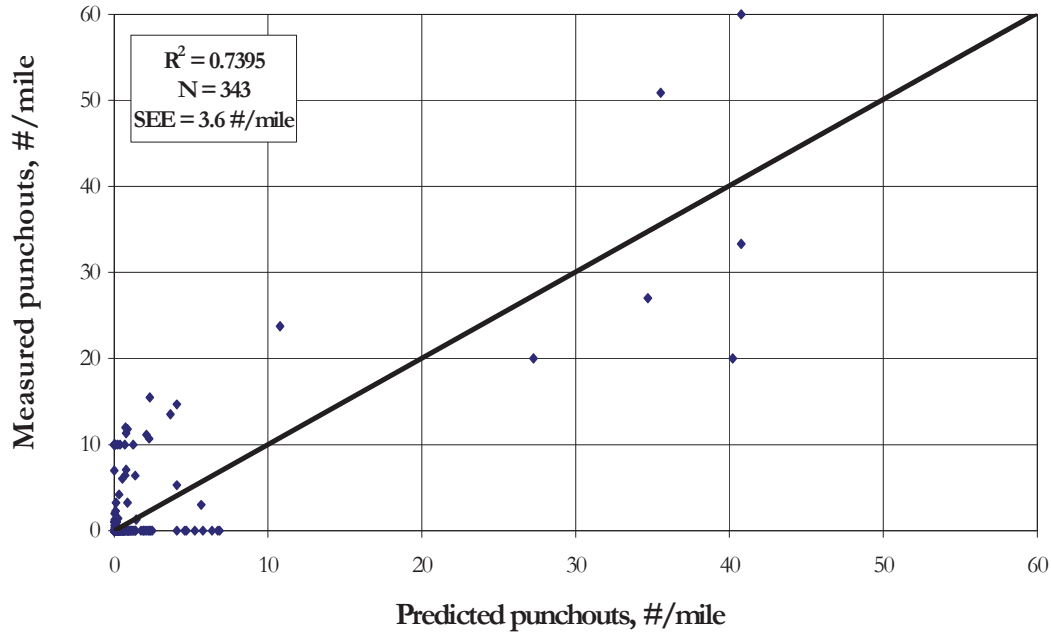


**Figure 5-17.** Comparison of Measured and Predicted Punchouts for New CRCP Resulting from Global Calibration Process

#### 5.4.4 Longitudinal Slab Cracking—SJPCP on Flexible Pavements

Bottom-up longitudinal fatigue cracking in the wheel paths is predicted as the primary structural distress in accordance with the procedure developed by Li and Vanderbossche (17). Critical bending stresses occur when the truck axle approaches the transverse joint of the slabs in both wheel paths. The wheel paths occur between the longitudinal joints (which are typically spaced from 5–8 ft depending on lane width), as illustrated in Figure 5-18. Similar to conventional JPCP design, calculation of critical stresses was done using neural nets (for speed) that require the slab and lower layer to be combined into an “equivalent slab” thickness based on equivalent stresses (load and temperature/moisture gradients) and contact friction between slab and base. This is done monthly as these parameters change over time.

A critical tensile bending stress occurs at the bottom of the slab under the wheel load, which increases when there is a high positive temperature gradient through the slab (the top of the slab is warmer than the bottom of the slab). Repeated loadings of heavy axles under those conditions result in fatigue damage along the bottom transverse joint of the slab (the point of maximum fatigue damage is computed), which eventually results in a longitudinal crack that propagates to the surface of the slab and along the slab. Bottom-up longitudinal cracking is calculated as a percent of the total number of slabs in the wheel paths, which is the output performance criteria used for structural design. This distress is predicted using the following globally calibrated Equation 5-37 for bottom-up longitudinal fatigue cracking:

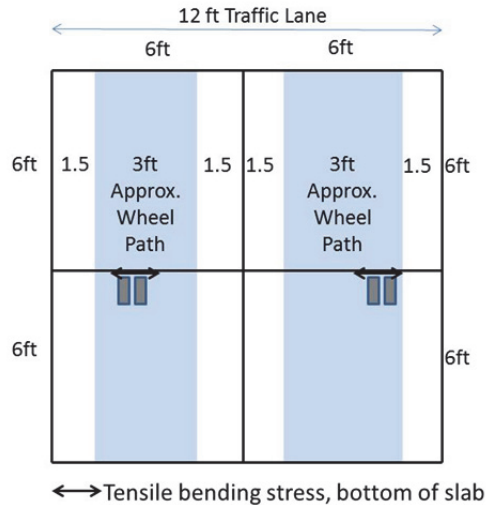


**Figure 5-18.** Illustration of Proper Location of Longitudinal Joints to Avoid Overlap with Truck Wheel Paths (to Avoid Corner Cracking) and the Resulting Critical Bending Stresses at Bottom of Slab That Are Considered to Limit Longitudinal Fatigue Cracking

$$LCRK = \frac{1}{1 + C_4 (DI_F)^{C_5}} \quad (5-37)$$

where:

$LCRK$  = Predicted amount of bottom-up longitudinal fatigue cracking, %

$DI_F$  = Fatigue damage calculated using the procedure described in this section (fraction from 0 to >1) at the most critical point along the transverse joint

$C_4, C_5$  = Global calibration constants ( $C_4 = 0.40$  and  $C_5 = -2.21$ )

The fatigue damage calculation is a process of summing damage from each damage increment at several critical points across the bottom of the slab along the transverse joint. The general expression for fatigue damage accumulation considering all critical factors for SJPCP longitudinal cracking is Equation 5-38 and referred to as Miner's hypothesis:

$$DI_F = \sum \frac{n_{i,j,k,l,m,n,o}}{N_{i,j,k,l,m,n,o}} \quad (5-38)$$

where:

$DI_F$  = Total fatigue damage (bottom-up)

$n_{i,j,k,\dots}$  = Applied number of load applications at condition  $i, j, k, l, m, n$

$N_{i,j,k,\dots}$  = Allowable number of load applications at condition  $i, j, k, l, m, n$

$i$  = Age (accounts for change in PCC modulus of rupture and elasticity, slab/AC contact friction)

$j$  = Month (accounts for change in AC dynamic modulus and dynamic subgrade K-Value)

$k$  = Axle type (single, tandem, and tridem for bottom-up cracking)

$l$  = Load level (incremental load for each axle type)

- $m$  = Equivalent temperature difference between top and bottom PCC surfaces
- $n$  = Traffic offset path (normal distribution)
- $o$  = Hourly truck traffic fraction

The applied number of load applications ( $n_{i,j,k,l,m,n}$ ) is the actual number of axle type,  $k$ , of load level,  $l$ , that passed through traffic pattern,  $n$ , under each condition  $i, j$ , and  $m$  (age, season, and temperature difference). The allowable number of load applications (to cracking  $N_{i,j,k,l,m,n}$ ) is the number of load cycles at which fatigue cracking is expected on average and is a function of the applied stress and PCC strength. The allowable number of load applications ( $N_{i,j,k,l,m,n}$ ) to cracking is determined using Equation 5-39 and applied to the PCC field fatigue Equation 5-38 to calculate the DI:

$$\log(N_{i,j,k,l,m,n}) = C_1 \cdot \left( \frac{MR_i}{\sigma_{i,j,k,l,m,n}} \right)^{C_2} - 0.4371 \tag{5-39}$$

where:

- $N_{i,j,k,\dots}$  = Allowable number of load applications at condition  $i, j, k, l, m, n$
- $MR_i$  = PCC modulus of rupture at age  $i$ , psi
- $\sigma_{i,j,k,\dots}$  = Applied stress at condition  $i, j, k, l, m, n$
- $C_1$  = Calibration constant, 2.0
- $C_2$  = Calibration constant, 1.22

A plot of measured longitudinal cracking versus the computed fatigue damage at the bottom of the PCC slab is shown in Figure 5-19. This plot follows the typical S-shaped curve and is termed the transfer function between slab longitudinal fatigue cracking and cumulative fatigue damage at the bottom of the slab.

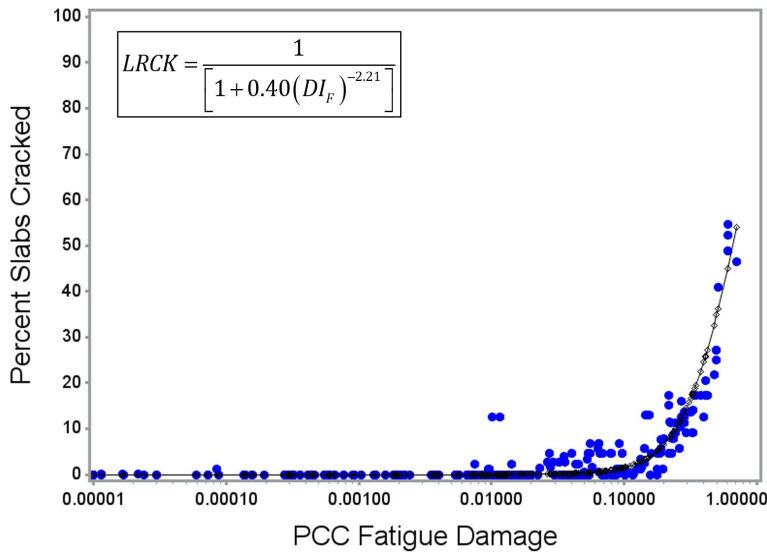


**Figure 5-19.** Measured Longitudinal Fatigue Cracking (LCRK) versus PCC Fatigue Damage (DIF) at Bottom of PCC Slab

A plot of measured versus predicted longitudinal cracking and the statistics resulting from the global calibration process is shown in Figure 5-20. Statistical hypothesis testing at the 0.05 significance level for the slope of the line (equal to 1.0), intercept (equal to 0), and for prediction bias (either over or under prediction) were not significant.

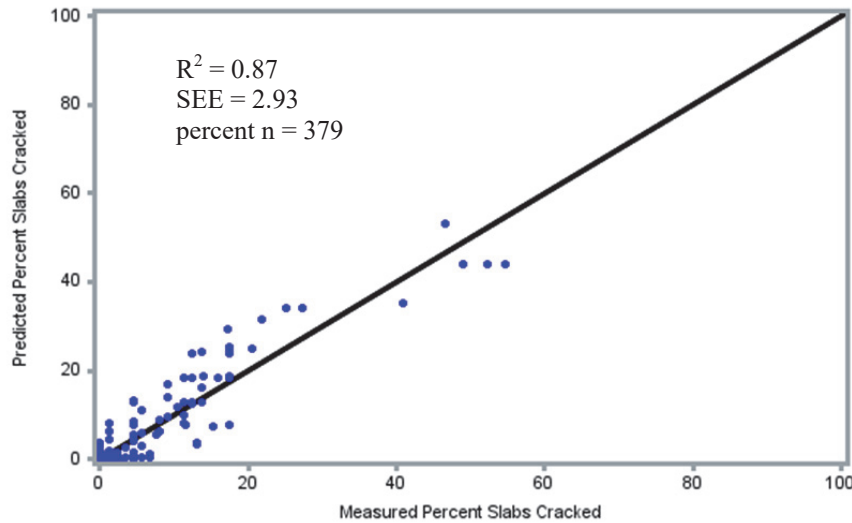


**Figure 5-20.** Comparison of Measured and Predicted Percentage SJPCP Overlay Slabs Longitudinally Cracked Resulting from Global Calibration Process

The standard error (or standard deviation of the residual error) for the percentage of slabs longitudinally cracked prediction global equation is shown in Equation 5-40.

$$s_{e(LCRACK)} = 3.5522 * LCRACK^{0.4315} + 0.5000 \quad (5-40)$$

where:

$LCRACK$  = Predicted longitudinal fatigue cracking based on mean inputs (corresponding to 50% reliability), percentage of slabs

$s_{e(LCRACK)}$  = Standard error of the estimate of longitudinal fatigue cracking at the predicted level of mean longitudinal cracking

#### 5.4.5 Smoothness—JPCP

In AASHTOWare Pavement ME Design, smoothness is predicted as a function of the initial as-constructed profile of the pavement and any change in the longitudinal profile over time and traffic due to distresses and foundation movements. The IRI model was calibrated and validated using LTPP field data to assure that it would produce valid results under a variety of climatic and field conditions. The following is the final calibrated model:

$$IRI = IRI_i + J1 * CRK + J2 * SPALL + J3 * TFAULT + J4 * SF \quad (5-41a)$$

where:

$IRI$  = Predicted IRI, in./mi

$IRI_i$  = Initial smoothness measured as IRI, in./mi

$CRK$  = Percent slabs with transverse cracks (all severities)

$SPALL$  = Percentage of joints with spalling (medium and high severities)

$TFAULT$  = Total joint faulting cumulated per mi, in.

$J1 = 0.8203$

$J2 = 0.4417$

$J3 = 1.4929$

$J4 = 25.24$

$SF$  = Site factor

$$SF = AGE (1 + 0.5556 * FI) (1 + P_{200}) * 10^{-6} \quad (5-41b)$$

where:

$AGE$  = Pavement age, yr

$FI$  = Freezing index, °F-days

$P_{200}$  = Percent subgrade material passing No. 200 sieve

The transverse cracking and faulting are obtained using the models described earlier. The transverse joint spalling is determined in accordance with Equation 5-41c, which was calibrated using LTTP and other data.

$$SPALL = \left[ \frac{AGE}{AGE + 0.01} \right] \left[ \frac{100}{1 + 1.005^{(-12 * AGE + SCF)}} \right] \quad (5-41c)$$

where:

$SPALL$  = Percentage joints spalled (medium- and high-severities)

$AGE$  = Pavement age since construction, yr

$SCF$  = Scaling factor based on site, design, and climate

$$SCF = -1400 + 350 \cdot AC_{PCC} \cdot (0.5 + PREFORM) + 43.4 f_c'^{0.4} - 0.2 (FT_{cycle} \cdot AGE) + 43 H_{PCC} - 536 WC_{PCC} \quad (5-41d)$$

$AC_{PCC}$  = PCC air content, %

$AGE$  = Time since construction, yr

$PREFORM$  = 1 if preformed sealant is present; 0 if not

$f_c'$  = PCC compressive strength, psi

$FT_{cycle}$  = Average annual number of freeze-thaw cycles

$H_{PCC}$  = PCC slab thickness, in.

$WC_{PCC}$  = PCC water/cement ratio

Model Statistics for Equation 5-41d are listed below:

$$R^2 = 78 \%$$

$$SEE = 6.8 \%$$

$$N = 179$$

A plot of measured versus predicted IRI values (smoothness) for new JPCP and the statistics from the global calibration is shown in Figure 5-21. The standard error for the initial JPCP IRI is 5.4 (in./mi). The equation for the standard error of predicted mean JPCP is shown in Equation 5-42.

$$s_{eJPCP\_IRI\_model} = 29.03 \ln(IRI) - 103.8 \quad (5-42)$$

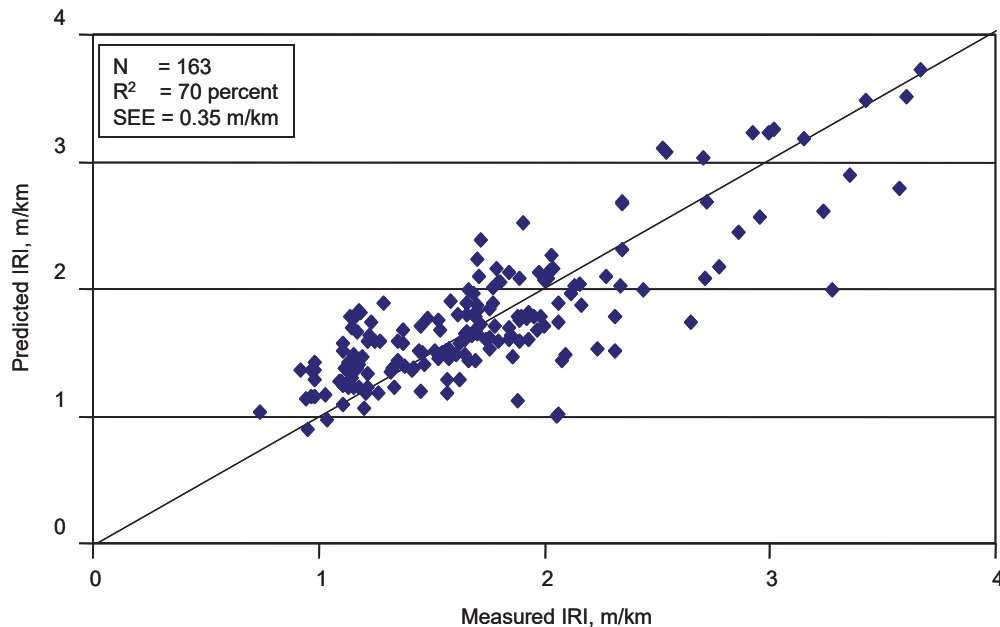


**Figure 5-21.** Comparison of Measured and Predicted IRI Values for New JPCP Resulting from Global Calibration Process

#### 5.4.6 Smoothness—CRCP

Smoothness change in CRCP is the result of a combination of the initial as-constructed profile of the pavement and any change in the longitudinal profile over time and traffic due to the development of distresses and foundation movements. Key distresses affecting the IRI for CRCP include punchouts. The global IRI model for CRCP is given as follows:

**Table 9-8.** Models Relating Material Index and Strength Properties to  $M_r$  (21)

Strength/ Index Property	Model	Comments	Test Standard
CBR	$M_r = 2555(\text{CBR})^{0.64}$ $M_r$ , psi	CBR = California Bearing Ratio, %	AASHTO T 193, "The California Bearing Ratio"
R-value	$M_r = 1155 + 555R$ $M_r$ , psi	R = R-value	AASHTO T 190, "Resistance R-Value and Expansion Pressure of Compacted Soils"
AASHTO layer coefficient	$M_r = 30,000 \left( \frac{a_i}{0.14} \right)$ $M_r$ , psi	$a_i$ = AASHTO layer coefficient	<i>AASHTO Guide for the Design of Pavement Structures</i>
PI and gradation*	$\text{CBR} = \frac{75}{1 + 0.278(P_{200}PI)}$	$P_{200}$ = percent passing No. 200 sieve size PI = plasticity index, %	AASHTO T 27, "Sieve Analysis of Coarse and Fine-Aggregates" AASHTO T 90, "Determining the Plastic Limit and Plasticity Index of Soils"
DCP*	$\text{CBR} = \frac{292}{\text{DCP}^{1.12}}$	CBR = California Bearing Ratio, % DCP = DCP index, mm/blow	ASTM D6951, "Standard Test Method for Use of the Dynamic Cone Penetrometer in Shallow Pavement Applications"

\* Estimates of CBR are used to estimate  $M_r$ .

### Interface Friction between Bound Layers

Layer interface friction is an input parameter to the AASHTOWare PMED, but is difficult to define and measure. Cores and visual surveys are used to determine if debonding exists along the project. Slippage cracks and two adjacent layers separating during the coring process may be a result of low interface friction between two AC layers. If these conditions are found to exist along a project, the designer could consider assuming no bond or a low interface friction during the rehabilitation design using the AASHTOWare PMED software, if those layers are to remain in place and not be milled or removed.

All of the global calibration efforts for flexible pavements, however, were completed assuming full friction between all layers—an interface friction value of 1.0 in the AASHTOWare PMED software. This value could be used unless debonding is found. Interface friction values less than 1.0 will increase rutting and cracking of the AC layers. The decrease in rutting and cracking of AC is minimal until the condition of full bond, a value of 1.0, is used. Thus, friction can be defined for just two conditions without significantly affecting the accuracy of the answer—fully bonded (a value of 1.0) or no bond (a value of 0). It should be noted that incomplete bonding is a condition

that should be limited and that the use of milling down to a stable layer is recommended in practice.

JPCP allows the user to define the PCC-base contact friction with a simple true/false statement. A statement of false designates no contact friction. A statement of true designates no slippage between layers and requires the user to input “Months until friction loss.” Calibration results for new or reconstructed JPCP showed that full contact friction existed over the life of the pavements for all base types, with the exception of CTB or lean concrete where extraordinary efforts were made to debond the layers. For this situation, the months of full contact friction were reduced to a range of 0–100 years, with a default value equal to the design life, to match the cracking exhibited. For new and reconstructed PCC designs, full friction should be assumed, unless debonding techniques are specified and confirmed through historical pavement construction records and defaults to 20 years, based on design life.

For rehabilitation of JPCP (CPR and overlays), full contact friction is input over the rehabilitation design life when cores through the base course show that an interface bond exists. Otherwise, the two layers are considered to have zero friction over the design life.

### Edge Drains

If the existing pavement has subsurface drains that remain in place, the outlets need to be found and inspected. Mini-cameras are used to inspect the edge drains and lateral lines to verify that they are free-flowing and not restricting the removal of water from the pavement structure.

### 9.2.8 Laboratory Tests for Materials Characterization of Existing Pavements

Table 9-6 provided a listing of the materials properties that must be measured to determine the inputs to the AASHTOWare PMED and to specify the condition of the existing pavement layers. Chapter 10 includes details on the testing of different pavement layers that is required in support of the MEPDG.

It is recommended that a sufficient laboratory test program to estimate the material properties of each layer is established as these are required inputs in accordance with the MEPDG. The following section lists the type of samples needed for measuring the properties of the in-place layers (refer to Table 9-5).

### AC Mixtures and Layers

- ♦ **Volumetric Properties** (air voids, asphalt content, gradation): Air voids (bulk specific and maximum theoretical specific gravities) of existing layers are obtained from as-built project records and used as input for Levels 1 and 2 (Table 9-2). The average effective asphalt content by volume and gradation measured during construction are used for the rehabilitation design. Selected cores recovered from the project are used to measure these properties whenever this volumetric data is unavailable from construction records. Samples recovered from 6-in.-diameter cores are used to ensure a sufficient amount of material for gradation tests. The ignition oven is used to measure the asphalt content (in accordance with AASHTO T 308 or an equivalent procedure) and then the gradation

on their unique needs and testing capabilities. The following provides more detailed discussion on determining the volumetric properties that are used to estimate these input parameters for new AC mixtures.

- † **Air Voids (AASHTO T 269),  $V_a$ :** The air voids at construction need to represent the average, in-place air voids expected after the AC has been compacted with the rollers, but prior to opening the roadway to truck traffic. This value will be unavailable during structural design because it has yet to be produced. It is recommended that this value be obtained from previous construction records for similar mixtures or the designer could enter the target value from the project specifications.
- † **Bulk Specific Gravity of the Combined Aggregate Blend (AASHTO T 84 and T 85),  $G_{sb}$ :** This value is dependent on the type of aggregates used in the AC and gradation. Most agencies will have an expected range of this value from previous mixture designs for the type of aggregates used, their source, and combined gradation (type of mixture dependent) specified for the project.
- † **Maximum Specific Gravity of Mixture (AASHTO T 209),  $G_{mm}$ :** This value is dependent on the type of aggregate, gradation, and asphalt content used in the AC. Most agencies will have an expected range of this value from previous mixture designs using the aggregate source and gradation (type of mixture) specified for the project. The maximum specific gravity can be calculated from the component properties if no historical information exists for the AC mixture specified for the project.
- † **Voids in Mineral Aggregate, VMA:** VMA is an input for thermal cracking predictions and determination of other volumetric properties. The mixture VMA needs to represent the condition of the mixture after it has been compacted with the rollers, but prior to opening the roadway to truck traffic. This value will be unavailable during structural design because it has yet to be produced and placed. It is recommended that the value be calculated from other volumetric properties that are obtained from construction records for similar type mixtures, aggregate sources, and gradations.
- † **Effective Asphalt Content by Volume,  $V_{be}$ :** The effective asphalt content by volume needs to represent the in-place asphalt content, after the mix has been placed by the paver. This value will be unavailable during structural design because it has yet to be produced. It is recommended that the value be calculated from the other volumetric properties, as shown in Table 10-3.

**Table 10-3.** Recommended Input Parameters and Values; Limited or No Testing Capabilities for AC (Input Levels 2 and/or 3)

Measured Property	Input Levels 2 or 3
Dynamic modulus, $E_{HMA}$ (new AC)	<ul style="list-style-type: none"> <li>• No dynamic modulus, <math>E_{AC}</math>, laboratory testing required.</li> <li>• Use MEPDG <math>E_{AC}</math> predictive equation. Inputs are gradation, asphalt viscosity, loading frequency, air void content, and effective bitumen content by volume. Input variables may be obtained through testing of lab prepared mix samples or from agency historical records.</li> <li>• Use typical <math>A_i</math>-<math>VTS</math>- values based on asphalt binder grade (PG, viscosity, or penetration grades).</li> </ul>
Dynamic modulus, $E_{HMA}$ (existing AC layer)	<ul style="list-style-type: none"> <li>• No dynamic modulus, <math>E_{AC}</math>, laboratory testing required.</li> <li>• Use MEPDG <math>E_{AC}</math> predictive equation. Inputs are gradation, bitumen viscosity, loading frequency, air void content, and effective bitumen content by volume. Input variables may be obtained through testing of extracted cores or from agency historical records.</li> <li>• Use typical <math>A_i</math>-<math>VTS</math>- values based on asphalt binder grade (PG, viscosity, or penetration grades).</li> <li>• Determine existing pavement condition rating (excellent, good, fair, poor, or very poor).</li> </ul>
Tensile strength, $TS$ (new AC surface; not required for existing AC layers)	<p>Use MEPDG regression equation:</p> $TS(\text{psi}) = 7416.712 - 114.016 * Va - 0.304 * Va^2 - 122.592 * VFA + 0.704 * VFA^2 + 405.71 * \log_{10}(Pen77) - 2039.296 * \log_{10}(A)$ <p>where:</p> <p><math>TS</math> = Indirect tensile strength at 14°F, psi  <math>Va</math> = HMA air voids, as-constructed, %  <math>VFA</math> = Voids filled with asphalt, as-constructed, %  <math>Pen77</math> = Asphalt penetration at 77°F, mm/10  <math>A</math> = Asphalt viscosity-temperature susceptibility intercept</p> <p>Input variables may be obtained through testing of lab prepared mix samples, extracted cores (for existing pavements), or from agency historical records.</p>

Continued on next page.

**Table 10-3.** Recommended Input Parameters and Values; Limited or No Testing Capabilities for AC (Input Levels 2 and/or 3), *continued*

Measured Property	Input Levels 2 or 3
Creep compliance, $D(t)$ (new AC surface; not required for existing AC layers)	Use MEPDG regression equation: $D(t) = D_1 * t^m$ $\log(D_1) = -8.524 + 0.01306 * T + 0.7957 * \log_{10}(Va) + 2.0103 * \log_{10}(VFA) - 1.923 * \log_{10}(A)$ $m = 1.1628 - 0.00185 * T - 0.04596 * Va - 0.01126 * VFA + 0.00247 * Pen_{77} + 0.001683 * T * Pen_{77}^{0.4605}$ where: $t$ = Time, months $T$ = Temperature at which creep compliance is measured, °F $Va$ = AC air voids, as-constructed, % $VFA$ = Voids filled with asphalt, as-constructed, % $Pen_{77}$ = Asphalt penetration at 77°F, mm/10 $A$ = Asphalt viscosity-temperature susceptibility intercept Input variables may be obtained through testing of lab prepared mix samples, extracted cores (for existing pavements), or from agency historical records.
Air voids	Use as-constructed mix type specific values available from previous construction records.
Effective volumetric asphalt content	Use as-constructed mix type specific values available from previous construction records. The percent asphalt content by weight is typically reported in mixture design and construction records. (The effective asphalt content by volume is equal to the VMA minus the air voids.)
Total unit weight	Use as-constructed mix type specific values available from previous construction records.

\*Note: AASHTOWare PMED software computes input Levels 2 and 3 dynamic modulus, tensile strength, creep compliance, etc. internally once; all the required input variables required by the various equation are provided.

*Continued on next page.*

**Table 10-3.** Recommended Input Parameters and Values; Limited or No Testing Capabilities for AC (Input Levels 2 and/or 3), *continued*

Measured Property	Recommended Level 3 Input																					
Poisson's ratio	<p>Use a predictive equation based on temperature included in the MEPDG for new AC mixtures and the typical values listed below for the existing AC layers:</p> <table border="1"> <thead> <tr> <th>Reference Temperature °F</th> <th>Dense-Graded AC (Level 3) <math>\mu_{\text{typical}}</math></th> <th>Open-Graded AC (Level 3) <math>\mu_{\text{typical}}</math></th> </tr> </thead> <tbody> <tr> <td>&lt; 0°F</td> <td>0.15</td> <td>0.35</td> </tr> <tr> <td>0–40°F</td> <td>0.20</td> <td>0.35</td> </tr> <tr> <td>40–70°F</td> <td>0.25</td> <td>0.40</td> </tr> <tr> <td>70–100°F</td> <td>0.35</td> <td>0.40</td> </tr> <tr> <td>100–130°F</td> <td>0.45</td> <td>0.45</td> </tr> <tr> <td>&gt;130°F</td> <td>0.48</td> <td>0.45</td> </tr> </tbody> </table>	Reference Temperature °F	Dense-Graded AC (Level 3) $\mu_{\text{typical}}$	Open-Graded AC (Level 3) $\mu_{\text{typical}}$	< 0°F	0.15	0.35	0–40°F	0.20	0.35	40–70°F	0.25	0.40	70–100°F	0.35	0.40	100–130°F	0.45	0.45	>130°F	0.48	0.45
Reference Temperature °F	Dense-Graded AC (Level 3) $\mu_{\text{typical}}$	Open-Graded AC (Level 3) $\mu_{\text{typical}}$																				
< 0°F	0.15	0.35																				
0–40°F	0.20	0.35																				
40–70°F	0.25	0.40																				
70–100°F	0.35	0.40																				
100–130°F	0.45	0.45																				
>130°F	0.48	0.45																				
Surface shortwave absorptivity	Use AASHTOWare Pavement ME Design default of 0.85.																					
Thermal conductivity	Typical values for asphalt concrete range from 0.244–2.0 Btu/(ft)(hr)(°F). Use the default value set in the program—1.25 Btu/(ft)(hr)(°F).																					
Heat capacity	Typical values for asphalt concrete range from 0.1–0.50 Btu/(lb)(°F). Use the default value set in the program—0.28 BTU/lb.-°F																					
Coefficient of thermal contraction	<p>Use the MEPDG predictive equation shown below:</p> $L_{MIX} = \frac{VMA * B_{ac} + V_{AGG} * B_{AGG}}{3 * V_{TOTAL}}$ <p>where:</p> <p><math>L_{MIX}</math> = Linear coefficient of thermal contraction of the AC mixture (1/°C)</p> <p><math>B_{ac}</math> = Volumetric coefficient of thermal contraction of the asphalt cement in the solid state (1/°C)</p> <p><math>B_{AGG}</math> = Volumetric coefficient of thermal contraction of the aggregate (1/°C)</p> <p>VMA = Volume of voids in the mineral aggregate, % (equals percent volume of air voids plus percent volume of asphalt cement, minus percent volume of absorbed asphalt cement)</p> <p><math>V_{AGG}</math> = Volume of aggregate in the mixture, %</p> <p><math>V_{TOTAL}</math> = 100%</p>																					

*Continued on next page.*

**Table 10-4.** PCC Material Input Level 1 Parameters and Test Protocols for New and Existing PCC, *continued*

Design Type	Measured Property	Source of Data		Recommended Test Protocol and/or Data Source
		Test	Estimate	
Existing intact and fractured PCC	Elastic modulus	X		ASTM C469 (extracted cores) AASHTO T 256 (non-destructive deflection testing)
	Poisson's ratio	X		ASTM C469 (extracted cores)
	Flexural strength	X		AASHTO T 97 (extracted cores)
	Unit weight	X		AASHTO T 121 (extracted cores)
	Surface shortwave absorptivity		X	National test protocol not available. Use AASHTOWare Pavement ME Design defaults
	Thermal conductivity	X		ASTM E1952 (extracted cores)
	Heat capacity	X		ASTM D2766 (extracted cores)

**Table 10-5.** Recommended Input Parameters and Values; Limited or No Test Capabilities for PCC Materials (Input Levels 2 or 3)

Measured Property	Recommended Input Levels 2 and 3									
New PCC elastic modulus and flexural strength	<ul style="list-style-type: none"> <li>• 28-day flexural strength <i>and</i> 28-day PCC elastic modulus, <i>or</i></li> <li>• 28-day compressive strength <i>and</i> 28-day PCC elastic modulus, <i>or</i></li> <li>• 28-day flexural strength <i>only</i>, <i>or</i></li> <li>• 28-day compressive strength <i>only</i></li> </ul>									
Existing intact PCC elastic modulus	Based on the pavement condition, select typical modulus values from the range of values given below: <table border="1" style="margin-left: 20px; width: 100%;"> <thead> <tr> <th>Qualitative Description of Pavement Condition</th> <th>Typical Modulus Ranges, psi</th> </tr> </thead> <tbody> <tr> <td>Adequate</td> <td><math>3-4 \times 10^6</math></td> </tr> <tr> <td>Marginal</td> <td><math>1-3 \times 10^6</math></td> </tr> <tr> <td>Inadequate</td> <td><math>0.3-1 \times 10^6</math></td> </tr> </tbody> </table>		Qualitative Description of Pavement Condition	Typical Modulus Ranges, psi	Adequate	$3-4 \times 10^6$	Marginal	$1-3 \times 10^6$	Inadequate	$0.3-1 \times 10^6$
Qualitative Description of Pavement Condition	Typical Modulus Ranges, psi									
Adequate	$3-4 \times 10^6$									
Marginal	$1-3 \times 10^6$									
Inadequate	$0.3-1 \times 10^6$									
Existing fractured PCC elastic modulus	The three common methods of fracturing PCC slabs include crack and seat, break and seat, and rubblization. In terms of materials characterization, cracked and seated or broken and seated PCC layers are considered a separate category from rubblized layers. At Level 3, typical modulus values may be adopted for design (see below): <table border="1" style="margin-left: 20px; width: 100%;"> <thead> <tr> <th>Fractured PCC Layer Type</th> <th>Typical Modulus Ranges, psi</th> </tr> </thead> <tbody> <tr> <td>Crack and Seat or Break and Seat</td> <td>150,00–1,000,000</td> </tr> <tr> <td>Rubblized</td> <td>50,000–150,000</td> </tr> </tbody> </table>		Fractured PCC Layer Type	Typical Modulus Ranges, psi	Crack and Seat or Break and Seat	150,00–1,000,000	Rubblized	50,000–150,000		
Fractured PCC Layer Type	Typical Modulus Ranges, psi									
Crack and Seat or Break and Seat	150,00–1,000,000									
Rubblized	50,000–150,000									

*Continued on next page.*

**Table 10-5.** Recommended Input Parameters and Values; Limited or No Test Capabilities for PCC Materials (Input Levels 2 or 3), *continued*

Measured Property	Recommended Input Levels 2 and 3																								
Poisson's ratio	Poisson's ratio for new PCC typically ranges between 0.10 and 0.21, with a value of 0.20 the default value assumed for PCC design. See below for typical Poisson's ratio values for PCC materials.																								
	<table border="1"> <thead> <tr> <th>PCC Materials</th> <th>Input Level 3 <math>\mu</math>typical</th> </tr> </thead> <tbody> <tr> <td>PCC Slabs (newly constructed or existing)</td> <td>0.20</td> </tr> <tr> <td>Fractured Slab:</td> <td></td> </tr> <tr> <td>    Crack/Seat</td> <td>0.20</td> </tr> <tr> <td>    Break/Seat</td> <td>0.20</td> </tr> <tr> <td>    Rubblized</td> <td>0.30</td> </tr> </tbody> </table>	PCC Materials	Input Level 3 $\mu$ typical	PCC Slabs (newly constructed or existing)	0.20	Fractured Slab:		Crack/Seat	0.20	Break/Seat	0.20	Rubblized	0.30												
	PCC Materials	Input Level 3 $\mu$ typical																							
	PCC Slabs (newly constructed or existing)	0.20																							
Fractured Slab:																									
Crack/Seat	0.20																								
Break/Seat	0.20																								
Rubblized	0.30																								
Unit weight	Select agency historical data or from the typical range for normal weight concrete: 140–160 lb/ft <sup>3</sup>																								
Coefficient of thermal expansion	Select agency historical values or typical values based on PCC coarse aggregate type.																								
	<table border="1"> <thead> <tr> <th>Aggregates Type</th> <th>Coefficient of Thermal Expansion (10<sup>-6</sup>/°F)</th> </tr> </thead> <tbody> <tr> <td>Andesite</td> <td>4.3</td> </tr> <tr> <td>Basalt</td> <td>4.3</td> </tr> <tr> <td>Diabase</td> <td>4.6</td> </tr> <tr> <td>Gabbro</td> <td>4.4</td> </tr> <tr> <td>Granite</td> <td>4.7</td> </tr> <tr> <td>Schist</td> <td>4.4</td> </tr> <tr> <td>Dolomite</td> <td>5.0</td> </tr> <tr> <td>Limestone</td> <td>4.3</td> </tr> <tr> <td>Quartzite</td> <td>5.2</td> </tr> <tr> <td>Sandstone</td> <td>5.3</td> </tr> <tr> <td>Expanded shale</td> <td>4.5</td> </tr> </tbody> </table>	Aggregates Type	Coefficient of Thermal Expansion (10 <sup>-6</sup> /°F)	Andesite	4.3	Basalt	4.3	Diabase	4.6	Gabbro	4.4	Granite	4.7	Schist	4.4	Dolomite	5.0	Limestone	4.3	Quartzite	5.2	Sandstone	5.3	Expanded shale	4.5
	Aggregates Type	Coefficient of Thermal Expansion (10 <sup>-6</sup> /°F)																							
	Andesite	4.3																							
	Basalt	4.3																							
	Diabase	4.6																							
	Gabbro	4.4																							
	Granite	4.7																							
	Schist	4.4																							
	Dolomite	5.0																							
	Limestone	4.3																							
	Quartzite	5.2																							
	Sandstone	5.3																							
Expanded shale	4.5																								
Surface shortwave absorptivity	Use the MEPDG default value of 0.85																								
Thermal conductivity	Typical values for PCC range from 0.2–2.0 Btu/(ft)(hr)(°F). Use the MEPDG default value—1.25 Btu/(ft)(hr)(°F).																								
Heat capacity	Typical values for PCC range from 0.1–0.50 Btu/(lb)(°F). Use the MEPDG default value—0.28 BTU/lb.-°F.																								

*Continued on next page.*

**Table 10-5.** Recommended Input Parameters and Values; Limited or No Test Capabilities for PCC Materials (Input Levels 2 or 3), *continued*

Measured Property	Recommended Input Levels 2 and 3																																																				
PCC set temperature	<p>Zero stress temperature, <math>T_z</math>, can be input directly or can be estimated from monthly ambient temperature and cement content using the equation shown below:</p> $T_z = (C_c * 0.59328 * H * 0.5 * 1000 * 1.8 / (1.1 * 2400) + MMT)$ <p>where:  <math>T_z</math> = PCC set temperature (allowable range: 70–212°F)  <math>C_c</math> = Cementitious content, lb/yd<sup>3</sup>  <math>H = -0.0787 + 0.007 * MMT - 0.00003 * MMT^2</math>  <math>MMT</math> = Mean monthly temperature for month of construction, °F</p> <p>An illustration of the zero stress temperatures for different mean monthly temperatures and different cement contents in the PCC mix design is presented below:</p> <table border="1"> <thead> <tr> <th rowspan="2">Mean Monthly Temperature, °F</th> <th rowspan="2">H</th> <th colspan="4">Cement Content, lbs/cy</th> </tr> <tr> <th>400</th> <th>500</th> <th>600</th> <th>700</th> </tr> </thead> <tbody> <tr> <td>40</td> <td>0.1533</td> <td>52</td> <td>56</td> <td>59</td> <td>62</td> </tr> <tr> <td>50</td> <td>0.1963</td> <td>66</td> <td>70</td> <td>74</td> <td>78</td> </tr> <tr> <td>60</td> <td>0.2333</td> <td>79</td> <td>84</td> <td>88</td> <td>93</td> </tr> <tr> <td>70</td> <td>0.2643</td> <td>91</td> <td>97</td> <td>102</td> <td>107</td> </tr> <tr> <td>80</td> <td>0.2893</td> <td>103</td> <td>109</td> <td>115</td> <td>121</td> </tr> <tr> <td>90</td> <td>0.3083</td> <td>115</td> <td>121</td> <td>127</td> <td>134</td> </tr> <tr> <td>100</td> <td>0.3213</td> <td>126</td> <td>132</td> <td>139</td> <td>145</td> </tr> </tbody> </table>	Mean Monthly Temperature, °F	H	Cement Content, lbs/cy				400	500	600	700	40	0.1533	52	56	59	62	50	0.1963	66	70	74	78	60	0.2333	79	84	88	93	70	0.2643	91	97	102	107	80	0.2893	103	109	115	121	90	0.3083	115	121	127	134	100	0.3213	126	132	139	145
Mean Monthly Temperature, °F	H			Cement Content, lbs/cy																																																	
		400	500	600	700																																																
40	0.1533	52	56	59	62																																																
50	0.1963	66	70	74	78																																																
60	0.2333	79	84	88	93																																																
70	0.2643	91	97	102	107																																																
80	0.2893	103	109	115	121																																																
90	0.3083	115	121	127	134																																																
100	0.3213	126	132	139	145																																																
Measured Property	Recommended Level 3 Input																																																				
Cement type	Estimate based on agency practices.																																																				
Cementitious material content	Estimate based on agency practices.																																																				
Water to cement ratio	Estimate based on agency practices.																																																				
Aggregate type	Estimate based on agency practices.																																																				
Curing method	Estimate based on agency practices.																																																				
Ultimate shrinkage	Estimate using MEPDG prediction equation.																																																				
Reversible shrinkage	Use MEPDG global default of 50 percent unless more accurate information is available.																																																				
Time to develop 50 percent of ultimate shrinkage	Use MEPDG global default of 35 days unless more accurate information is available.																																																				

*Note:* Project specific testing is not required at Level 3. Historical agencies test values assembled from past construction with tests conducted using the list protocols.

**Table 10-6.** Chemically Stabilized Materials Input Level 1 Requirements and Test Protocols for New and Existing Chemically Stabilized Materials

Design Type	Material Type	Measured Property	Source of Data		Recommended Test Protocol and/or Data Source	
			Test	Estimate		
New	Lean concrete and cement-treated aggregate	Elastic modulus	X		ASTM C469	
		Flexural strength (only required when used in AC pavement design)	X		AASHTO T 97	
	Lime-cement-fly ash stabilized material	Resilient modulus		X	No test protocols available. Estimate using Levels 2 and 3.	
	Soil cement	Resilient modulus	X		Mixture Design and Testing Protocol (MDTP) in conjunction with AASHTO T 307	
	Lime stabilized soil	Resilient modulus	X		Mixture Design and Testing Protocol (MDTP) in conjunction with AASHTO T 307	
	All	Unit weight			X	No testing required. Estimate using Levels 2 and 3.
		Poisson's ratio			X	No testing required. Estimate using Levels 2 and 3.
		Thermal conductivity		X		ASTM E1952
		Heat capacity		X		ASTM D2766
		Surface short wave absorptivity			X	No test protocols available. Estimate using Levels 2 and 3.
Existing	All	FWD backcalculated modulus	X		AASHTO T 256 & ASTM D5858 (see Section 9.3.4)	
		LTE Transverse Cracks	X		AASHTO T 256 & ASTM D5858 (see Section 9.3.4)	
	All	Unit weight			X	No testing required. Estimate using Levels 2 and 3.
		Poisson's ratio			X	No testing required. Estimate using Levels 2 and 3.
		Thermal conductivity		X		ASTM E1952 (cores)
		Heat capacity		X		ASTM D2766 (cores)
		Surface short wave absorptivity			X	No test protocols available. Estimate using Levels 2 and 3.

**Table 10-7.** Recommended Input Levels 2 and 3 Parameters and Values for Chemically Stabilized Material Properties

Required Input	Recommended Input Level																		
Elastic/ resilient modulus	Use unconfined compressive strength ( $f'_c$ or $q_u$ ) in psi of lab samples or extracted cores converted into elastic/resilient modulus by the following:																		
	<table border="1"> <thead> <tr> <th>Material</th> <th>Relationship for Modulus</th> <th>Test Method</th> </tr> </thead> <tbody> <tr> <td>Lean concrete and cement treated aggregate</td> <td><math>E = 57000(f'_c)^{0.5}</math></td> <td>AASHTO T 22</td> </tr> <tr> <td>Open graded cement stabilized aggregate</td> <td>Use input Level 3</td> <td>None</td> </tr> <tr> <td>Lime-cement-fly ash</td> <td><math>E = 500 + q_u</math></td> <td>ASTM C593</td> </tr> <tr> <td>Soil cement</td> <td><math>E = 1200(q_u)</math></td> <td>ASTM D1633</td> </tr> <tr> <td>Lime stabilized soil</td> <td><math>M_r = 0.124(q_u) + 9.98</math></td> <td>ASTM D5102</td> </tr> </tbody> </table>	Material	Relationship for Modulus	Test Method	Lean concrete and cement treated aggregate	$E = 57000(f'_c)^{0.5}$	AASHTO T 22	Open graded cement stabilized aggregate	Use input Level 3	None	Lime-cement-fly ash	$E = 500 + q_u$	ASTM C593	Soil cement	$E = 1200(q_u)$	ASTM D1633	Lime stabilized soil	$M_r = 0.124(q_u) + 9.98$	ASTM D5102
	Material	Relationship for Modulus	Test Method																
	Lean concrete and cement treated aggregate	$E = 57000(f'_c)^{0.5}$	AASHTO T 22																
	Open graded cement stabilized aggregate	Use input Level 3	None																
	Lime-cement-fly ash	$E = 500 + q_u$	ASTM C593																
	Soil cement	$E = 1200(q_u)$	ASTM D1633																
	Lime stabilized soil	$M_r = 0.124(q_u) + 9.98$	ASTM D5102																
	<i>or</i> Select typical $E$ and $M_r$ values in psi as follows:																		
	<table border="1"> <tbody> <tr> <td>Lean concrete, <math>E</math></td> <td>2,000,000</td> </tr> <tr> <td>Cement stabilized aggregate, <math>E</math></td> <td>1,000,000</td> </tr> <tr> <td>Open graded cement stabilized aggregate, <math>E</math></td> <td>750,000</td> </tr> <tr> <td>Soil cement</td> <td>500,000</td> </tr> <tr> <td>Lime-cement-fly ash, <math>E</math></td> <td>1,500,000</td> </tr> <tr> <td>Lime stabilized soil, <math>M_r</math></td> <td>45,000</td> </tr> </tbody> </table>	Lean concrete, $E$	2,000,000	Cement stabilized aggregate, $E$	1,000,000	Open graded cement stabilized aggregate, $E$	750,000	Soil cement	500,000	Lime-cement-fly ash, $E$	1,500,000	Lime stabilized soil, $M_r$	45,000						
Lean concrete, $E$	2,000,000																		
Cement stabilized aggregate, $E$	1,000,000																		
Open graded cement stabilized aggregate, $E$	750,000																		
Soil cement	500,000																		
Lime-cement-fly ash, $E$	1,500,000																		
Lime stabilized soil, $M_r$	45,000																		
Flexural strength (only required for flexible pavements)	Use 20 percent of compressive strength of lab samples or extracted cores as an estimate of the flexural strength for all chemically stabilized materials, <i>or</i> select typical $M_r$ values in psi as follows:																		
	<table border="1"> <tbody> <tr> <td>Chemically stabilized material placed under flexible pavement (base)</td> <td>750</td> </tr> <tr> <td>Chemically stabilized material used as subbase, select material, or subgrade under flexible pavement</td> <td>250</td> </tr> </tbody> </table>	Chemically stabilized material placed under flexible pavement (base)	750	Chemically stabilized material used as subbase, select material, or subgrade under flexible pavement	250														
	Chemically stabilized material placed under flexible pavement (base)	750																	
Chemically stabilized material used as subbase, select material, or subgrade under flexible pavement	250																		
Poisson's ratio	Select typical Poisson's ratio values as follows:																		
	<table border="1"> <tbody> <tr> <td>Lean concrete and cement stabilized aggregate</td> <td>0.1–0.2</td> </tr> <tr> <td>Soil cement</td> <td>0.15–0.35</td> </tr> <tr> <td>Lime-fly ash materials</td> <td>0.1–0.15</td> </tr> <tr> <td>Lime stabilized soil</td> <td>0.15–0.2</td> </tr> </tbody> </table>	Lean concrete and cement stabilized aggregate	0.1–0.2	Soil cement	0.15–0.35	Lime-fly ash materials	0.1–0.15	Lime stabilized soil	0.15–0.2										
	Lean concrete and cement stabilized aggregate	0.1–0.2																	
	Soil cement	0.15–0.35																	
	Lime-fly ash materials	0.1–0.15																	
Lime stabilized soil	0.15–0.2																		
Unit weight	Use the MEPDG default value of 150 pcf.																		
Thermal conductivity	Use the MEPDG default value of 1.25 BTU/h-ft-°F.																		
Heat capacity	Use the MEPDG default value of 0.28 BTU/lb-°F.																		

### 10.5 Unbound Aggregate Base Materials and Engineered Embankments

Similar to AC and PCC, physical and engineering properties are required for the unbound pavement layers and foundation. The physical properties include dry density, moisture content, and classification properties, while the engineering property includes the resilient modulus. Designers must be aware that the resilient modulus values have to be determined at the optimum moisture content and maximum dry density, thus ensuring the unbound layers are representative of conditions when the pavement is opened to truck traffic.

For new alignments or new designs, the MEPDG default resilient modulus values (input Level 3) may be used, the modulus may be estimated from other properties of the material (input Level 2), or the modulus may be measured in the laboratory (input Level 1). For rehabilitation or reconstruction designs, the resilient modulus of each unbound layer and embankment is backcalculated from deflection basin data or estimated from DCP or CBR tests. If the resilient modulus values are determined by backcalculating elastic layer modulus values from deflection basin tests, those values need to be adjusted to laboratory conditions (31, 32). Table 10-8 lists the values recommended in those design pamphlets. If the resilient modulus values are estimated from the DCP or other tests, those values may be used as inputs to the MEPDG, but should be checked based on local material correlations and adjusted to laboratory conditions, if necessary. The DCP test is performed in accordance with ASTM D6951 or an equivalent procedure. For compatibility, the dry density and water content should be representative of the condition of the soil in determining the resilient modulus.

**Table 10-8.** C-Values to Convert the Calculated Layer Modulus Values to an Equivalent Resilient Modulus Measured in the Laboratory

Layer Type	Location	C-Value or $M_r$ /EFWD Ratio
Aggregate Base/ Subbase	Between a stabilized and AC layer	1.43
	Below a PCC layer	1.32
	Below an AC layer	0.62
Subgrade- Embankment	Below a stabilized subgrade/embankment	0.75
	Below an AC or PCC layer	0.52
	Below an unbound aggregate base	0.35

Table 10-9 summarizes the input Level 1 parameters required for the unbound aggregate base, subbase, embankment, and subgrade soil material types listed in Table 10-1. The recommended test protocols are also listed in Table 10-9. Although input Level 1 is preferred for pavement design, most agencies are not equipped with the testing facilities required to characterize the paving materials. Thus, for the more likely situation where agencies have only limited or no testing capability for characterizing unbound aggregate base, subbase, embankment, and subgrade soil materials, input Levels 2 and 3 are recommended, which are provided in Table 10-10. For most analyses, it is permissible for designers to use a combination of Levels 1, 2, and 3 material inputs based on their unique needs and testing capabilities.

**Table 10-9.** Unbound Aggregate Base, Subbase, Embankment, and Subgrade Soil Input Level 1 Material Requirements and Test Protocols for New and Existing Materials

Design Type	Measured Property	Source of Data		Recommended Test Protocol and/or Data Source
		Test	Estimate	
New (lab samples) and existing (extracted materials)	Two Options:  Regression coefficients $k_1, k_2,$ and $k_3$ for the generalized constitutive model that defines resilient modulus as a function of stress state and regressed from laboratory resilient modulus tests.  Determine the average design resilient modulus for the expected in-place stress state from laboratory resilient modulus tests.	X		AASHTO T 307 or NCHRP 1-28A The MEPDG generalized model is as follows:  $M_r = k_1 p_a \left( \frac{\theta}{P_a} \right)^{k_2} \left( \frac{\tau_{oct}}{P_a} + 1 \right)^{k_3}$ where: $M_r$ = resilient modulus, psi $\theta$ = bulk stress $= \sigma_1 + \sigma_2 + \sigma_3$ $\sigma_1$ = major principal stress $\sigma_2$ = intermediate principal stress $\sigma_3$ = minor principal stress confining pressure $\tau_{oct}$ = octahedral shear stress $= \frac{1}{3} \sqrt{(\sigma_1 - \sigma_2)^2 + (\sigma_1 - \sigma_3)^2 + (\sigma_2 - \sigma_3)^2}$ $P_a$ = normalizing stress $k_1, k_2, k_3$ = regression constants
	Poisson's ratio		X	No national test standard, use MEPDG default values
	Maximum dry density	X		AASHTO T 180
	Optimum moisture content	X		AASHTO T 180
	Gradation	X		AASHTO T 88
	Specific gravity	X		AASHTO T 100
	Saturated hydraulic conductivity	X		AASHTO T 215
	Soil water characteristic curve parameters	X		Pressure plate (AASHTO T 99), or Filter paper (AASHTO T 180), or Tempe cell (AASHTO T 100)
Existing material to be left in place	FWD backcalculated modulus	X		AASHTO T 256 and ASTM D5858
	Poisson's ratio		X	No national test standard, use MEPDG default values

**Table 10-10.** Recommended Levels 2 and 3 Input Parameters and Values for Unbound Aggregate Base, Subbase, Embankment, and Subgrade Soil Material Properties

Required Input	Recommended Input Level			
Resilient modulus	Use Level 3 inputs based on the unbound aggregate base, subbase, embankment, and subgrade soil material AASHTO Soil Classification. AASHTO Soil Class is determined using the material gradation, plasticity index, and liquid limit.			
		Recommended Resilient Modulus at Optimum Moisture (AASHTO T 180), psi		
	AASHTO Soil Classification	Base/Subbase for Flexible and Rigid Pavements	Embankment and Subgrade for Flexible Pavements	Embankment and Subgrade for Rigid Pavements
	A-1-a	40,000	29,500	18,000
	A-1-b	38,000	26,500	18,000
	A-2-4	N/A	24,500	16,500
	A-2-5	N/A	21,500	16,000
	A-2-6	N/A	21,000	16,000
	A-2-7	N/A	20,500	16,000
	A-3	N/A	16,500	16,000
	A-4	N/A	16,500	15,000
	A-5	N/A	15,500	8,000
	A-6	N/A	14,500	14,000
	A-7-5	N/A	13,000	10,000
A-7-6	N/A	11,500	13,000	
	<p>Note: (1) The resilient modulus is converted to a k-value within the software when evaluating rigid pavements. (2) The resilient modulus values at the time of construction for the same AASHTO soil classification are different under flexible and rigid pavements because the stress-state under these pavements is different. Soils are stress dependent and the resilient modulus will change with changing stress-state (refer to Table 10-9). The above default values can be used assuming the soils are at the maximum dry density and optimum water content as defined from AASHTO T 180. (3) Only A-1-a and A-1-b soils are used as base courses.</p>			
Maximum dry density	Estimate using the following inputs: gradation, plasticity index, and liquid limit.			
Optimum moisture content				
Specific gravity				
Saturated hydraulic conductivity				
Soil water characteristic curve parameters	Select based on aggregate/subgrade material class.			

adequacy of the trial design) and the desired level of reliability. Next, AASHTOWare PMED is used to process the input data. Data processing includes estimating climate-related aspects, such as the pavement temperature profile for each analysis period using the EICM and computing long-term PCC flexural strength, as discussed in Subsection 5.3.

Next, the processed data is used to perform a design analysis by computing pavement structural responses (stress, deflections) required for each distress type incrementally. Computed structural responses are used in transfer functions to estimate distress and smoothness.

The trial rehabilitation design is then evaluated for adequacy using prescribed performance criteria at the given reliability level. Trial designs deemed inadequate are modified and reevaluated until a suitable design is achieved. Design modifications could range from making simple changes to JPCP overlay thickness, varying joint spacing, varying PCC strength, or adopting a new rehabilitation strategy altogether.

The design process for rehabilitation design with JPCP overlays or CPR of existing JPCP is very similar to new or reconstructed JPCP design. Some exceptions are noted in the sections below.

#### *Performance Prediction Models*

The globally calibrated performance models for new pavements apply to rehabilitation design.

#### *Materials Inputs*

In terms of materials inputs, the key difference between new and rehabilitation design is that the latter deals with characterizing in situ materials properties along with those for the overlay. A description of the material inputs for existing pavement layers and how to estimate them is presented in Chapter 9.

#### *Selection of Design Features*

The choice of design features is restricted to those variables being introduced as part of the rehabilitation. For most rehabilitated JPCP design situations, the pavement design features are a combination of the existing design features and new features introduced as part of rehabilitation. Selecting the appropriate design features for the rehabilitated JPCP is key to achieving a successful design. Guidance on how to select the right design features is presented in Table 12-12.

### **Design Modifications to Reduce Distress for JPCP Rehabilitation**

Trial designs with excessive amounts of predicted distress/smoothness need to be modified to reduce predicted distress/smoothness to tolerable values (within the desired reliability level). Some of the most effective ways of accomplishing this are listed in Table 12-13.

**Table 12-12.** Guidance on How to Select the Appropriate Design Features for Rehabilitated JPCP Design

Type of JPCP Rehabilitation	Specific Rehabilitation Treatments	Recommendation on Selecting Design Feature
<b>Concrete Pavement Restoration (CPR)</b>	Diamond grinding	Select initial smoothness (IRI) based on agency grinding specifications and values typically achieved on CPR projects. If significant settlements/heaves exist, the initial IRI should be set higher than new/reconstruction design.
	Load transfer restoration (LTR)	Select load transfer mechanism based on the type of retrofit load transfer mechanism installed (e.g., 1.5-in. dowels). For situations where LTR was not applied, the existing JPCP LTE must be assessed. Existing doweled JPCP with very poor LTE may be considered undoweled.
	Shoulder repair, retrofit, or replacement	A new edge support condition reflective of the repairs, retrofit, or replacement applied. For example, if an existing asphalt shoulder is replaced with tied PCC shoulders, the rehabilitated design must reflect this change in edge support. Also, where no shoulder repair is carried out, the condition of the current shoulder must be considered in characterizing edge support conditions.
	Retrofit edge drains	The rehabilitated JPCP design should reflect improved drainage conditions by upgrading the base erodibility.
	Full-depth repairs or slab replacement	The effect on full-depth repairs and/or slab replacement on existing damage and future cracking estimates must be fully accounted for.
<b>Unbonded JPCP overlay</b>	Separation layer	An AC separator layer prevents reflection of underlying joints and cracks, provides a highly erosion-resistant material, and provides sufficient contact friction so that joints will form in the JPCP overlay. The JPCP overlay behaves structurally as if it is built on a strong, non-erodible “base” course consisting of the AC separation layer and the existing slab. The program structurally combines the JPCP overlay and the AC separator layer into an equivalent slab. Full contact friction interface should be input over the entire design life. The AC material must be specified to be extremely resistant to stripping.
	Existing PCC condition	The existing PCC overall condition must be considered in selecting the appropriate layer elastic modulus. This is done by adjusting backcalculated or lab-tested estimates of elastic modulus with a damage factor determined by the existing JPCP visual condition.
	JPCP overlay	Selection of design features for the JPCP overlay (including shoulder type and slab width) is similar to that outlined for new design in Chapter 10 of this manual.

*Continued on next page.*

**Table 12-12.** Guidance on How to Select the Appropriate Design Features for Rehabilitated JPCP Design, *continued*

Type of JPCP Rehabilitation	Specific Rehabilitation Treatments	Recommendation on Selecting Design Feature
<b>Bonded JPCP overlay</b>	PCC overlay	Design features must reflect the condition of the existing pavement, as very few pre-overlay repairs are typically done for this rehabilitation.
<b>JPCP overlay over existing flexible pavement</b>	JPCP overlay	<p>Selection of design features for the JPCP overlay (including shoulder type and slab width) is similar to that outlined for new or reconstructed design in Chapter 10. Condition of existing flexible pavement is characterized using one of the three hierarchical input levels:</p> <ul style="list-style-type: none"> <li>✦ Level 1 rehabilitation calculates the existing damage based on the FWD back-calculated modulus.</li> <li>✦ Level 2 calculates the damage based on the existing fatigue cracking from a visual distress survey.</li> <li>✦ Level 3 calculates the damage based on a condition rating as Excellent, Good, Fair, Poor, or Very Poor, as defined in Table 12-10.</li> </ul> <p>For all rehabilitation levels, the dynamic modulus, <math>E_{HMS}</math>, is adjusted to reflect the magnitude of damage within the existing asphalt layers. The existing AC layer now becomes the base course in the analysis mod. Full friction should be input over the full design life of the concrete overlay.</p>
<b>Bonded concrete overlay of asphalt (SJPCP)</b>	Short jointed bonded concrete overlay of asphalt pavement	<p>The longitudinal joint spacing is a very critical input. Joint spacing can vary from 5–8 ft, depending on lane width. A critical design principle is to not locate a longitudinal joint in the truck wheel path. This design procedure does not consider heavy loads traveling down the longitudinal joint that create corner cracks. This design procedure considers truck wheel paths that travel between the longitudinal joints, where tensile bending stresses are calculated at the bottom of the PCC slabs and used in the fatigue damage calculation for PCC thickness design.</p> <p>Transverse joint load transfer efficiency (LTE) can be varied from 25–95 percent and from season to season. An annual value of 80 percent is recommended as typical from FWD load transverse efficiency for this type of overlay. All sections were calibrated at 80 percent LTE.</p>

*Continued on next page.*

**Table 12-12.** Guidance on How to Select the Appropriate Design Features for Rehabilitated JPCP Design, *continued*

Type of JPCP Rehabilitation	Specific Rehabilitation Treatments	Recommendation on Selecting Design Feature
<b>Bonded concrete overlay of asphalt (SJPCP) (continued)</b>	Short jointed bonded concrete overlay of asphalt pavement <i>(continued)</i>	Condition of existing flexible pavement is a preselected Level 2 input at 65 percent fatigue cracking. Calibration of the longitudinal cracking model indicated that a large proportion of the sections showed some reduction in contact friction over service life between the PCC and AC layers. The use of 65 percent cracking was the approach selected to provide a reasonable input to the design. It effectively reduced the equivalent slab thickness to calculate the appropriate bending stress in the bottom of the PCC slab.

**Table 12-13.** Recommendations for Modifying Trial Design to Reduce Distress/Smoothness for JPCP Rehabilitation Design

Distress Type	Recommended Modifications to Design
<b>Faulting</b>	<ul style="list-style-type: none"> <li>✦ <b>Include dowels or increase diameter of dowels.</b> This is applicable to both restored JPCP and non-doweled JPCP overlays. The use of properly sized dowels is generally the most reliable and cost-effective way to control joint faulting. A slight increase of diameter of the dowels (i.e., 0.25 in.) will significantly reduce the mean steel-to-PCC bearing stress and thus the joint faulting.</li> <li>✦ <b>Improve subsurface drainage.</b> This is applicable to both restored JPCP and JPCP overlays. Subsurface drainage improvement for rehabilitated pavements basically consists of providing retrofit edge-drains and other related facilities. A permeable separator layer (usually asphalts or chemically stabilized) can be used to improve drainage of unbonded JPCP over existing rigid pavements. Studies have shown that subsurface drainage improvement with retrofit edge-drains can reduce faulting, especially for non-doweled JPCP. This is considered in design by reducing the amount of precipitation infiltrating into the pavement structure.</li> <li>✦ <b>Widen the traffic lane slab by 1–2 ft.</b> This is applicable to JPCP overlays. Widening the slab effectively moves the wheel load away from the slab corner, greatly reducing the deflection of the slab and the potential for erosion and pumping. Studies have shown that slab widening can reduce faulting by about 50 percent.</li> </ul>

*Continued on next page.*

**Table 12-13.** Recommendations for Modifying Trial Design to Reduce Distress/Smoothness for JPCP Rehabilitation Design, *continued*

Distress Type	Recommended Modifications to Design
<b>Faulting</b> ( <i>continued</i> )	<ul style="list-style-type: none"> <li>✦ <b>Decrease joint spacing.</b> This is applicable to JPCP overlays over existing flexible pavements and unbonded JPCP overlays. Shorter joint spacing generally results in smaller joint openings, making aggregate interlock more effective and increasing joint LTE.</li> <li>✦ <b>Erodibility of separator layer.</b> This is mostly only applicable to unbonded JPCP overlays. It may be applicable to the leveling course placed during the construction of JPCP overlays of existing flexible pavements. Specifying a non-erodible AC material or a geotextile as the separator reduces the potential for base/underlying layer erosion and, consequently, faulting.</li> </ul>
<b>Transverse cracking</b>	<ul style="list-style-type: none"> <li>✦ <b>Increase slab thickness.</b> This is only applicable to JPCP overlays. Thickening the overlay slab is an effective way to decrease critical bending stresses both from truck axle loads and from temperature differences in the slab. Field studies have shown that thickening the slab can reduce transverse cracking significantly. At some thickness, however, a point of diminishing returns is reached and fatigue cracking does not decrease significantly.</li> <li>✦ <b>Decrease joint spacing.</b> This is only applicable to JPCP overlays. A shorter joint spacing results in lower curling stresses in the slab. This effect is very significant, even over the normal range of joint spacing for JPCP, and should be considered a critical design feature.</li> <li>✦ <b>Increase PCC strength (and concurrent change in PCC elastic modulus and CTE).</b> This is applicable only to JPCP overlays. By increasing the PCC strength, the modulus of elasticity also increases, thereby reducing its effect. The increase in modulus of elasticity will actually increase the critical bending stresses in the slab. There is probably an optimum PCC flexural strength for a given project that provides the most protection against fatigue damage.</li> <li>✦ <b>Widen the traffic lane slab by 2 ft.</b> This is applicable to rehabilitation with overlays. Widening the slab effectively moves the wheel load away from the longitudinal free edge of the slab and greatly reduces the critical bending stress and potential for transverse cracking.</li> </ul>

*Continued on next page.*

**Table 12-13.** Recommendations for Modifying Trial Design to Reduce Distress/Smoothness for JPCP Rehabilitation Design, *continued*

Distress Type	Recommended Modifications to Design
<b>Transverse cracking</b> ( <i>continued</i> )	<ul style="list-style-type: none"> <li>✦ <b>Add a tied PCC shoulder (monolithically placed with the traffic lane).</b> This is applicable to rehabilitation with or without overlays. The use of a monolithically placed tied-PCC shoulder that has the properly sized tie-bars is generally an effective way to reduce edge bending stress and reduce transverse cracking. A PCC shoulder that is placed after the traffic lane does not generally produce high LTE and significantly reduced bending stresses over the design period.</li> </ul>
<b>Longitudinal Fatigue Cracking</b>	<ul style="list-style-type: none"> <li>✦ Increase slab thickness (8 in. maximum)</li> <li>✦ Increase existing AC layer thickness</li> <li>✦ Increase PCC strength (and concurrent change in PCC elastic modulus and CTE)</li> <li>✦ Tied PCC shoulder</li> </ul>
<b>Smoothness</b>	<ul style="list-style-type: none"> <li>✦ <b>Build smoother pavements initially and minimize distress.</b> The smoothness prediction model shows that smoothness loss occurs mostly from the development of distresses such as cracking, faulting, and spalling. Minimizing or eliminating such distresses by modifying trial design properties that influence the distresses would result in a smoother pavement. Hence, all of the modifications discussed in previous sections (for cracking and faulting) are applicable to improving smoothness.</li> </ul>

### 12.3.5 CRCP Rehabilitation Design

A brief description of the CRCP rehabilitation designs options is described in this section.

- ✦ **Unbonded CRCP overlay of existing rigid pavement:** Unbonded CRCP ( $\geq 7$  in. thick) placed on existing intact concrete pavement (JPCP, JRCP, or CRCP), existing composite pavement, or fractured PCC pavement. Unbonded overlays must have a separator layer similar to that described for unbonded JPCP overlays (see paragraph 12.3.3).
- ✦ **Bonded PCC overlay of existing CRCP:** Bonded PCC overlays over existing CRCP involve the placement of a thin concrete layer atop the prepared existing CRCP to form a permanent monolithic CRC section.
- ✦ **CRCP overlay of existing flexible pavement:** Conventional CRCP overlays ( $> 7$  in. thick) can be applied to existing flexible pavements. When subjected to axle loads, the CRCP overlaid flexible pavement behaves similarly to a new CRCP with an asphalt base course.

## Design Considerations

- ✦ **Performance criteria:** Performance indicators used for CRCP rehabilitation design are crack width, LTE, punchouts, and smoothness.
- ✦ **Design reliability:** Handled in the same manner as new designs (see Chapter 7).
- ✦ **Factors that affect distress:** A detailed description of the factors that affect the performance indicators to CRCP rehabilitation design are presented in Table 12-14. By selecting the appropriate values of these factors, designers may reduce specific distress and improve overall pavement performance.

### Trial Rehabilitation with CRCP Designs

The rehabilitation design process described under Subsection 12.3.3 for JPCP rehabilitation design is valid for CRCP as well. The performance prediction models for new CRCP are also valid for CRCP overlays. Further, as with JPCP rehabilitation, selecting the appropriate design features for the rehabilitated CRCP is key to achieving a successful design. For most rehabilitated CRCP design situations, the pavement design features are a combination of the existing design features and new features introduced as part of rehabilitation. Guidance on how to select the appropriate design features is presented in Table 12-15.

### Design Modifications to Reduce Distress for CRCP Overlays

Crack width, longitudinal reinforcement percentage, slab thickness, and support conditions are the primary factors affecting CRCP performance and punchout development. Hence, modifying the factors that influence them is the most effective manner of reducing punchouts and smoothness loss. Crack spacing cannot be modified for bonded PCC over existing CRCP.

**Table 12-14.** Summary of Factors that Influence Rehabilitated CRCP Distress and Smoothness

Parameter	Comment
<b>Transverse crack width and spacing</b>	Transverse crack width is very critical to CRCP performance. It plays a dominant role in controlling the degree of load transfer capacity provided at the transverse cracks. It is strongly influenced by the reinforcement content, PCC shrinkage, construction PCC set temperature, and PCC CTE. Smaller crack widths increase the capacity of the crack for transferring repeated shear stresses (caused by heavy axle loads) between adjacent slab segments over the long term. Wider cracks exhibit lower LTE over time and traffic, which results in increased load-related critical tensile stresses at the top of the slab, followed by increased fatigue damage and punchouts. A maximum crack width of 0.02 in. over the design life is recommended.
<b>Transverse crack LTE</b>	The LTE of transverse cracks is a critical factor in controlling the development of punchout related longitudinal cracking. Maintaining a load transfer of 95 percent or greater (through aggregate interlock over the CRC overlay design life) will limit the development of punchout distress. This is accomplished by limiting crack width over the entire year, especially the cold months.

*Continued on next page.*

**Table 12-14.** Summary of Factors that Influence Rehabilitated CRCP Distress and Smoothness, *continued*

Parameter	Comment
<b>Lane to shoulder longitudinal joint load transfer</b>	The load transfer of the lane to shoulder joint affects the magnitude of the tensile bending stress at the top of the slab (between the wheel loads in a transverse direction). It is a critical pavement response parameter that controls the development of longitudinal cracking between adjacent transverse cracks and, consequently, the development of punchouts. The use of design features that could provide and maintain adequate edge support throughout the pavement rehabilitation design life is therefore key to adequate performance.
<b>Overlay CRC thickness</b>	From the standpoint of slab stiffness, this is an important design feature that has a very significant influence on performance. Note that for bonded PCC over existing CRCP, the equivalent stiffness of the overlay and existing PCC layer is used in analysis. In general, as the slab thickness of a CRC overlay increases, the capacity to resist critical bending stress increases, as does the slab's capability to transfer load across the transverse cracks. Consequently, the rate of development of punchouts decreases and smoothness loss is reduced.
<b>Amount of longitudinal reinforcement and depth of reinforcement</b>	<p>Longitudinal steel reinforcement is an important design parameter because it is used to control the opening of the transverse cracks for unbonded CRCP overlays and CRCP overlays over existing flexible pavement. Also, the depth at which longitudinal reinforcement is placed below the surface greatly affects crack width. It is recommended that longitudinal steel reinforcement be placed above mid-depth in the slab.</p> <p>For bonded PCC over existing CRCP, the amount of reinforcement entered into the models is the same as that of the existing CRCP because cracks are already formed and no reinforcement is placed in the overlay PCC. Depth of the steel reinforcement is equal to the depth to the reinforcement in the existing CRCP (ignore the overlay PCC thickness because cracks are already formed through the slabs).</p>
<b>Slab width</b>	Slab width has typically been synonymous with lane width (usually 12 ft). Widened lanes are typically 13–14 ft. Field and analytical studies have shown that the wider slab keeps truck axles away from the free edge, greatly reducing tensile bending stresses (in the transverse direction) at the top slab surface and deflections at the lane-shoulder joint. This has a significant effect on reducing the occurrence of edge punchouts. This design procedure does not directly address CRCP with widened slabs but can be approximately modeled by shifting the mean lateral load position by the width of slab widening.

**Table 12-15.** Guidance on How to Select the Appropriate Design Features for Rehabilitated CRCP Design.

Type of CRCP Rehabilitation	Specific Rehabilitation Treatments	Recommendation on Selecting Design Feature
<b>Unbonded CRCP overlay</b>	Interlayer placement	An adequate asphalt separator layer is very important for a CRCP overlay, because it ensures that no working joints or cracks in the existing pavement will reflect upward through the CRCP. This normally requires 1 in. of AC, but if joints with poor LTE exist, a thicker AC layer may be necessary. The AC separator layer should have normal contact friction with the CRCP overlay and the existing PCC layer in order to improve the structural capacity of the pavement. Erodibility of the separation layer is calculated based upon properties of the AC separation layer. (This utilizes percent asphalt by volume.
<b>Unbonded CRCP overlay (continued)</b>	Interlayer placement (continued)	If this separation layer is permeable with a typically very low asphalt content, the designer must adjust the percent asphalt to a value of 11 percent.)
	Existing PCC condition	The existing PCC overall condition must be considered when selecting the appropriate layer elastic modulus. This is done by adjusting backcalculated or lab-tested estimates of elastic modulus with a damage factor determined by existing CRCP visual condition.
	CRCP overlay	Selection of design features for the CRCP overlay (including shoulder type and slab width) is similar to that outlined for new/reconstruction design in Chapter 10.
<b>Bonded PCC overlay on CRCP</b>	PCC bonded overlay	The existing CRCP surface must be prepared and a new PCC overlay bonded on top. The only joint that needs sawing is the longitudinal lane-to-lane joint, which should be sawed completely through, plus 0.5 in. This bonded PCC design is unusual but has performed well in a number of projects in Texas and elsewhere. Design input features must reflect the condition of the existing CRCP.
<b>CRCP overlay over existing flexible pavement</b>	CRCP overlay	Selection of design features for the CRCP overlay (including shoulder type and slab width) is similar to that outlined for new or reconstructed design in Chapter 10. Condition of existing flexible pavement is rated as Excellent, Good, Fair, Poor, or Very Poor, as described in Table 12-10. These ratings will result in adjustments to the dynamic modulus, $E_{AC}$ , of the existing AC layer that now becomes the base course. The lower the rating the larger the downward adjustment of $E^*$ of the existing AC layer.

- ✦ **Increase overlay slab thickness.** An increase in CRCP slab thickness will reduce punchouts based on a decrease in critical tensile fatigue stresses at the top of the slab and an increase in crack shear capability. There is also a greater tolerance to maintain a high load transfer capability at the same crack width, allowing for reduced tensile stress at top of the slab.
- ✦ **Increase percent longitudinal reinforcement in overlay.** Even though an increase in steel content will reduce crack spacing, it has been shown to greatly reduce punchouts overall due to narrower cracks widths.
- ✦ **Reduce the PCC set temperature** (when PCC sets) through improved curing procedure (water curing). The higher the PCC set temperature, the wider the crack openings at lower temperatures.
- ✦ **Reduce the depth of reinforcement in overlay.** This is applicable only to unbonded CRCP overlay and CRCP over existing flexible pavement. Placement of steel closer to the pavement surface reduces punchouts by keeping cracks tighter. (However, to avoid construction problems and limit infiltration of chlorides, do not place closer than 3.5 in. from the surface.)
- ✦ **Increase PCC tensile strength.** Increasing the CRCP tensile strength decreases the fatigue damage and, consequently, punchouts. However, it must be noted that there is a corresponding increase in PCC elastic modulus that increases the magnitude of stresses generated within the PCC, somewhat reducing the benefit of increased tensile strength.
- ✦ **Reduce the coefficient of thermal expansion of overlay PCC.** Use of a lower thermal coefficient of expansion concrete will reduce crack width opening for the same crack spacing.
- ✦ **Increase AC separator layer thickness.** The thicker the separator layer, the less sensitive the overlay is to deterioration in the existing pavement. For badly deteriorated existing pavements, thick ( $\geq 3$  in. thick) AC separator layers are recommended for CRCP overlays.
- ✦ **Reduction in PCC shrinkage.** Reducing the cement content and improved curing are two ways to reduce ultimate shrinkage.

### 12.3.6 Additional Considerations for Rehabilitation with PCC

There are several important considerations that need to be addressed as part of rehabilitation design to ensure adequate performance of the rehabilitation design throughout its design life. These issues include:

- ✦ Shoulder reconstruction
- ✦ Subdrainage improvement
- ✦ CPR/pre-overlay repairs
- ✦ Separator layer design (for unbonded JPCP/CRCP over existing rigid pavements)

- ✦ Joint design (for JPCP overlays)
- ✦ Reflection crack control (for bonded PCC over existing JCPC/CRCP)
- ✦ Bonding (for bonded PCC overlays over existing JPCP/CRCP)
- ✦ Guidelines for the addition of traffic lanes
- ✦ Guidelines for the widening of narrow traffic lanes

This page intentionally left blank.

**Table 13-3.** Guidance for Modifying AC Trial Designs to Satisfy Performance Criteria

Distress and IRI	Design Feature Revisions to Minimize or Eliminate Distress
<b>Alligator cracking (bottom initiated)</b>	<ul style="list-style-type: none"> <li>✦ Increase the thickness of AC layers</li> <li>✦ For thicker AC layers (&gt; 5 in.), increase the dynamic modulus</li> <li>✦ For thinner AC layers (&lt; 3 in.), reduce the dynamic modulus</li> <li>✦ Revise the mixture design of the AC base layer (increase the percent crushed aggregate, use manufactured fines, increase the asphalt content, use a harder asphalt but ensure that the same percent compaction level is achieved along the roadway, use a polymer-modified asphalt, etc.)</li> <li>✦ Increase the density and reduce the air void of the AC base layer</li> <li>✦ Increase the resilient modulus of the aggregate base (increase density, reduce plasticity, reduce amount of fines, etc.)</li> </ul>
<b>Thermal transverse cracking</b>	<ul style="list-style-type: none"> <li>✦ Use softer asphalt in the surface layer</li> <li>✦ Reduce the creep compliance of the AC surface mixture</li> <li>✦ Increase the indirect tensile strength of the AC surface mixture</li> <li>✦ Increase the asphalt content of the surface mixture</li> </ul>
<b>Rutting in AC</b>	<ul style="list-style-type: none"> <li>✦ Increase the dynamic modulus of the AC layers</li> <li>✦ Use a polymer-modified asphalt in the layers near the surface</li> <li>✦ Increase the amount of crushed aggregate</li> <li>✦ Increase the amount of manufactured fines in the AC mixtures</li> <li>✦ Reduce the asphalt content in the AC layers</li> </ul>
<b>Rutting in unbound layers and subgrade</b>	<ul style="list-style-type: none"> <li>✦ Increase the resilient modulus of the aggregate base and increase the density of the aggregate base</li> <li>✦ Stabilize the upper foundation layer for weak, frost-susceptible, or swelling soils, and use thicker granular layers</li> <li>✦ Place a layer of select embankment material with adequate compaction</li> <li>✦ Increase the AC thickness</li> </ul>
<b>IRI AC</b>	<ul style="list-style-type: none"> <li>✦ Require more stringent smoothness criteria and greater incentives (building the pavement smoother at the beginning)</li> <li>✦ Improve the foundation and use thicker layers of non-frost-susceptible materials</li> <li>✦ Stabilize any expansive soils</li> <li>✦ Place a subsurface drainage system to remove groundwater</li> </ul>

*Continued on next page.*

**Table 13-3.** Guidance for Modifying AC Trial Designs to Satisfy Performance Criteria, *continued*

<b>Distress and IRI</b>	<b>Design Feature Revisions to Minimize or Eliminate Distress</b>
<b>Longitudinal fatigue cracking (surface initiated)</b>	<p><i>Note:</i> It is recommended to not use the surface-initiated crack prediction equation as a design criterion until the critical pavement response parameter and prediction methodology has been verified. Refer to Chapter 3. The cumulative damage and longitudinal cracking transfer function (Equations 5-5 and 5-8) should be used with caution when making design decisions (in terms of longitudinal cracking, or top-down cracking) regarding the adequacy of a trial design.</p> <ul style="list-style-type: none"> <li>+ Reduce the dynamic modulus of the AC surface course</li> <li>+ Increase AC thickness</li> <li>+ Use softer asphalt in the surface layer</li> <li>+ Use a polymer-modified asphalt in the surface layer; AASHTOWare Pavement ME Design does not adequately address the benefit of PMA mixtures</li> </ul>
<b>Reflection cracking</b>	<ul style="list-style-type: none"> <li>+ Increase AC overlay thickness</li> <li>+ Increase the modulus of the AC overlay</li> </ul>

**Note:** Index page numbers are based on the original third edition; they have not been updated to reflect any errata repagination.

## Index

### A

AADTT (Annual Daily Truck Traffic) 95  
AASHTOWare Pavement ME Design.  
    *See* AASHTOWare PMED  
AASHTOWare PMED 1, 20, 36  
    axle-load distributions 97  
    distress prediction 40  
    inputs 217  
    predicted performance values 220–222  
    required inputs 6, 33  
    supplemental information 219–220  
    three-stage process 3  
    TTC groups 100  
absolute error 133  
AC (asphalt concrete) 1. *See* asphalt concrete  
accumulated damage 19  
aggregate base 20  
aggregate gradation 143  
air voids 145  
alkali silica reactivity (ASR) 27  
alligator cracking 35, 46, 166, 220  
    area, calculating 48  
analysis 1  
    interval 39  
    of pavement evaluation data 130–137  
    three-stage process 3  
    trial design 7–9  
Annual Daily Truck Traffic (AADTT) 95  
annual modulus 165  
AREA method 134  
asphalt binder 12  
asphalt classification 129  
asphalt concrete (AC) 1  
    design inputs 123  
    differences, design 4  
    existing pavements 185–186  
    laboratory tests 128–129  
    layers, number of 166  
    leveling courses 192  
    material property inputs 141–149  
    milling 125  
    overlays 22–23, 184  
    pavement types 20–22  
    performance indicators 18, 35–36  
    pre-overlay treatment 182  
    reflective cracks of 55  
    rehabilitation 177–192  
    test protocols 12  
    trenching 125  
    trial design, modifying 191, 223–224  
    volumetric properties 128

asphalt content by volume 145  
asphalt materials 140  
asphalt shingles (RAS) 142  
asphalt treated permeable base (ATPB) 28, 165, 166  
ASR (alkali silica reactivity) 27  
assessment, existing pavement 109–113  
    checklist 111–113  
    steps and activities 114  
ATPB (asphalt treated permeable base) 28, 165, 166  
Atterberg limits 159  
axle-load  
    configuration 99  
    distribution 19, 96–98  
    lateral wander 102  
    spectra 33–34

### B

backcalculation procedures 18, 132–133  
base course 168  
base erodibility 171  
BCOA (Bonded Concrete Overlays of Asphalt pavements) 24  
bedrock 140, 169  
Best Fit method 134  
Bonded Concrete Overlays of Asphalt pavements (BCOA) 24  
borings 124  
bottom-up cracking 35  
    longitudinal 37, 77–80  
    transverse 36  
break and seat 185  
bulk specific gravity 145

### C

calibration  
    coefficients 20  
    factors 1, 31, 40  
California bearing ratio (CBR) value 126. *See* CBR value  
CAM (cement aggregate mixtures) 20  
candidate repair treatments 181  
CBR value 126  
cement aggregate mixtures (CAM) 20, 28  
cementitious materials 20  
cement treated base (CTB) 20, 28  
    fatigue cracks, calculating 50  
classification, asphalt 129  
climate 102–103  
climatic effects 19  
climatic loading 17

compacted embankment 164  
 composite pavements 20  
 Concrete Pavement Restoration (CPR) 85, 203, 208  
 condition assessment, existing pavements 109–113  
   checklist 111–113  
   steps and activities 114  
 condition survey 115  
 construction  
   month 31, 85  
   new 2  
   staged 29  
 contact friction 169–170  
 continuously reinforced concrete pavement (CRCP) 18, 23  
   analysis parameters 187–189  
   design inputs 121  
   distress factors 212, 213  
   modifications 212  
   overlays 24  
   performance criteria, AC overlays 190  
   predicted performance values 221–222  
   punchouts 74–75  
   rehabilitation 198, 212  
   slab width 174  
   smoothness 82, 226  
   trial design 168  
   trial design, modifying 191  
 conventional flexible pavements 20  
 cores 124  
 corner deflections 68  
 CPR (Concrete Pavement Restoration) 85, 203, 208  
 crack  
   width 226  
 crack and seat 185  
 cracking  
   asphalt concrete (AC) pavements 35  
   comparison, measured and predicted 53–54  
   existing slab 188  
   load and non-load 29  
   Portland cement concrete (PCC) pavements 36  
   spacing 172, 221  
   width 173, 221  
 CRCP (continuously reinforced concrete pavement).  
   See continuously reinforced concrete pavement  
 creep compliance 42, 129  
   asphalt materials 143–144  
 criteria, performance indicator 6  
 CTB (cement treated base). See cement treated base  
 cumulative damage 1  
   index 32, 47  
 curing time 86

## D

damaged modulus 183  
 data collection, field 119  
 DCP (dynamic cone penetrometer) testing 122, 126  
 D-cracking 27  
 deep strength flexible pavements 20  
 deflection basin tests 18, 116, 122  
   spacing 123  
 deflections 1, 17  
 dense-graded base course 168  
 design 1  
   direction, trucks in 95  
   inputs, grouping 6  
   lane, trucks in 95  
   life 32, 85  
   modifications, JPCP 207  
   performance criteria 31–32, 87–88  
   process, elements 17  
   reliability 6, 32, 88–89  
   three-stage process 3  
 design reliability 205, 212, 217  
 design strategy  
   flexible pavements 20–23, 161–167  
   overlay 21–22  
   rigid pavement 23–26  
   trial 6  
 destructive tests 18, 116, 124–128  
   cores and borings 124  
   edge drains 128  
   in-place strength 126  
   interface friction 127–128  
   summary 125  
 deterioration 183  
 developing calibration factors 1  
 differential energy, cumulative 69  
 distress  
   prediction models 27, 40  
   reducing 191  
   rehabilitated JPCP 205–206  
   rehabilitating CRCP 212  
   types and severity levels 131  
 Distress Identification Manual 118, 122  
 distribution factors, truck traffic 99  
 drainage systems 18, 23, 162, 164–165  
 dry density 159  
 dual tire spacing 27, 102  
 dynamic cone penetrometer (DCP) testing 122, 126.  
   See DCP (dynamic cone penetrometer)  
   testing  
 dynamic modulus 19, 42, 129, 188, 200  
   asphalt materials 143

## E

early-age opening 29